The Structure, Evolution and Dynamics of a Nocturnal Convective System Simulated Using the WRF-ARW Model

Ben Blake

IMSG at NOAA/NCEP/EMC

EMC Seminar

29 March 2016

Outline

- Motivation/Background
- Brief Overview of 3-4 June 2013 MCS
- Model Configuration
- Control Simulation and Sensitivity Tests
- System Structure and Evolution
  - Advection by the LLJ
  - Surface vs. Elevated Cold Pool
  - Variation in structure around the cold pool
- Application of Theories to Variation in Structure
  - RKW framework
  - Wave theory framework
- Conclusions and Future Work

Motivation

- There is a pronounced nocturnal maximum in thunderstorm activity across the central US (e.g. Kincer 1916; Palmen & Newton 1969; Wallace 1975)
- Nocturnal convection has been difficult to represent in NWP and climate models (Surcel et al. 2010), although convection-allowing models have demonstrated some skill (Davis et al. 2003; Clark et al. 2007)
- Convection at night over this region is often elevated (Wilson & Roberts 2006)
- A framework governing nocturnal, elevated convection is lacking (Trier et al. 2006) in contrast to surface-based convection (e.g. Rotunno et al. 1988)

Diurnal Variations in Warm Season Thunderstorm Frequency

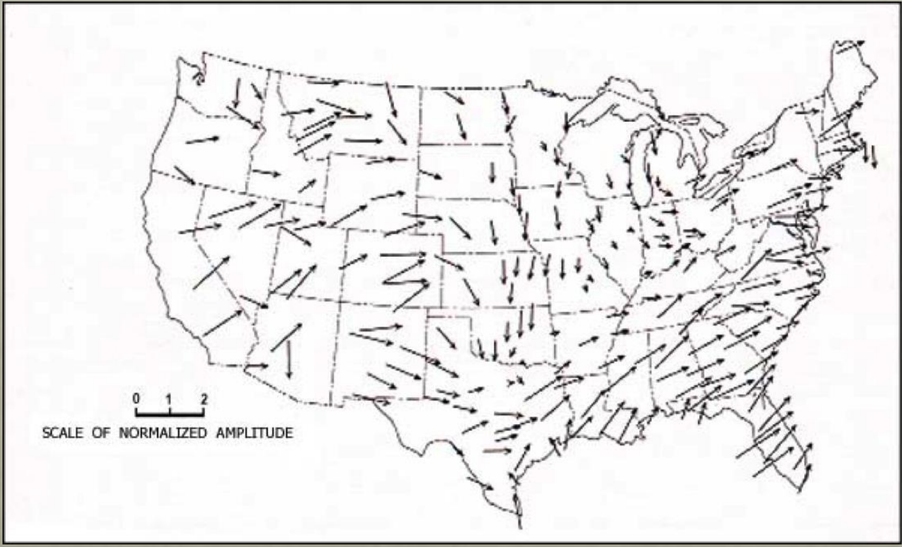

Figure from Wallace and Hobbs (1977)

Conditions Associated with Nocturnal Convection

- Stable Boundary Layer
- Low-Level Jet (e.g. Blackadar 1957; Holton 1967; Shapiro et al. 2015)
  - Positively correlated with rainfall intensity (e.g. Arritt et al. 1997; Tuttle and Davis 2006)
  - Frontal overrunning (e.g. Trier and Parsons 1993)
  - Convergence (e.g. Pu and Dickinson 2014)
- Elevated Terrain to the West (e.g. Carbone et al. 2002; Ahijevych et al. 2004)
  - Mountain-Plains Solenoidal Circulation (e.g. Wolyn and McKee 1994)
  - PV Anomalies (e.g. Li and Smith 2010)
- Mesoscale Convective Vortices (e.g. Raymond and Jiang 1990)
- Gravity Waves (e.g. Lindzen and Tung 1976; Fovell et al. 2006)
- Bores (e.g. Rottman and Simpson 1989)

Gravity Waves vs. Bores

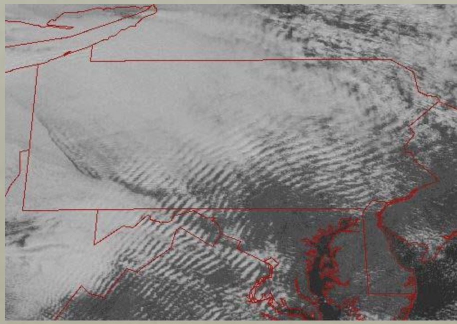

- Gravity waves – ubiquitous in atmosphere; generated when force of gravity or buoyancy tries to restore equilibrium
  - Penetration of stable layers by convection
  - Primarily result in upward transport of momentum
  - Ducted gravity waves can travel large horizontal distances from their source

- Bores – a type of gravity wave response that can be generated as a gravity current comes into contact with a low-level stable layer (e.g. Rottman & Simpson 1989, Koch et al. 1991)
  - Intense upward displacements of air parcels (~0.5-1.5 km) in the lowest ~3 km
  - At the surface, passage accompanied by a hydrostatic pressure jump and no appreciable change in temperature or slight warming

Refer to Markowski & Richardson (2010) and listed papers for more information

Study Goals

- This study focuses on a high-resolution, convection-allowing simulation of a nocturnal MCS over the southern Great Plains during 3-4 June 2013
- Nocturnal MCS occurred well to the south of a quasi-stationary frontal boundary
  - Allows insight into mechanisms responsible for nocturnal convection apart from frontal ascent
- System transitioned from surface-based to elevated as the boundary layer stabilized
- Low-level jet develops and waves/bores are present
- **Main Goal:** To advance the knowledge of the dynamics, structure, and evolution of nocturnal convection
- Applied two dynamical frameworks to a 3-D system (most case studies of bores utilized a 2-D framework)

3-4 June 2013
Large-Scale Synoptic Context

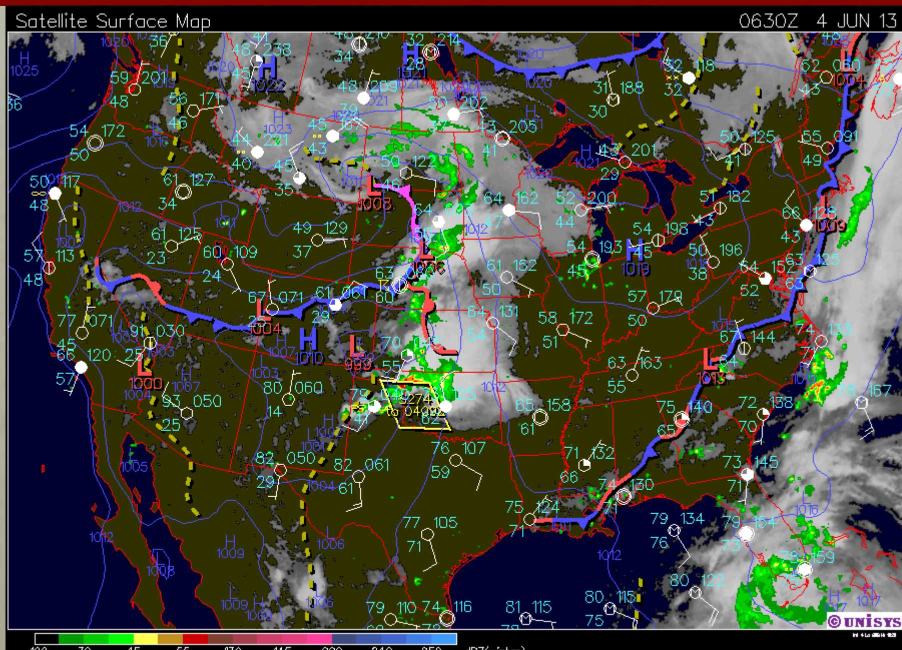

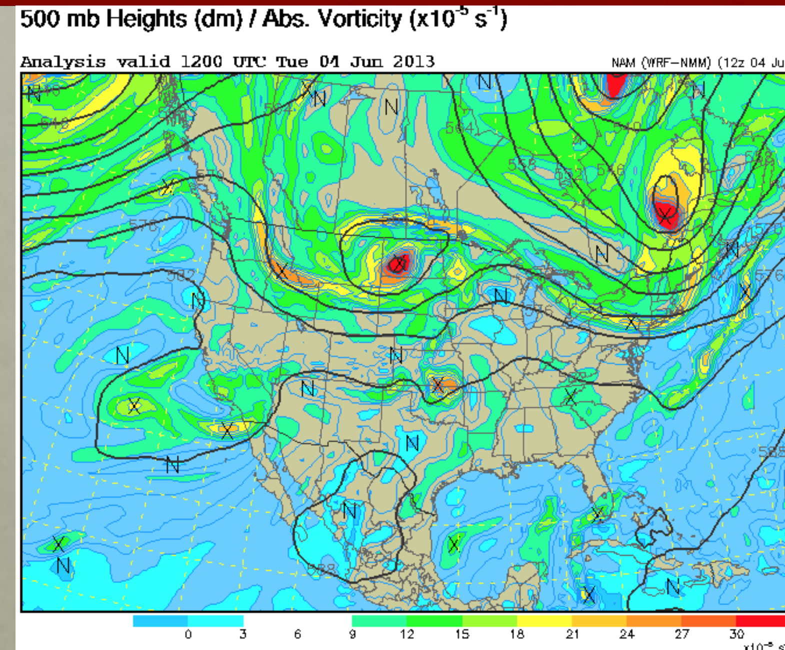

- Cyclonic vorticity maximum and associated shortwave trough
- Warm front moves NE through W OK & TX panhandle – became a quasi-stationary front in KS
- Dryline develops around 1900 UTC 3 June across OK & TX panhandles – remains quasi-stationary

3-4 June 2013
Mesoscale Features

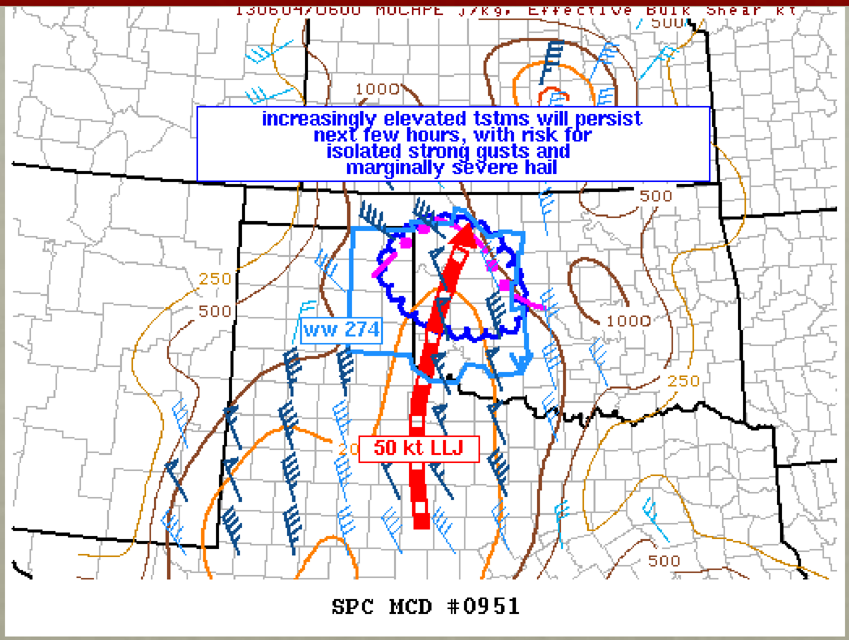

0500 UTC 500 m CAPE (RAP Analysis)

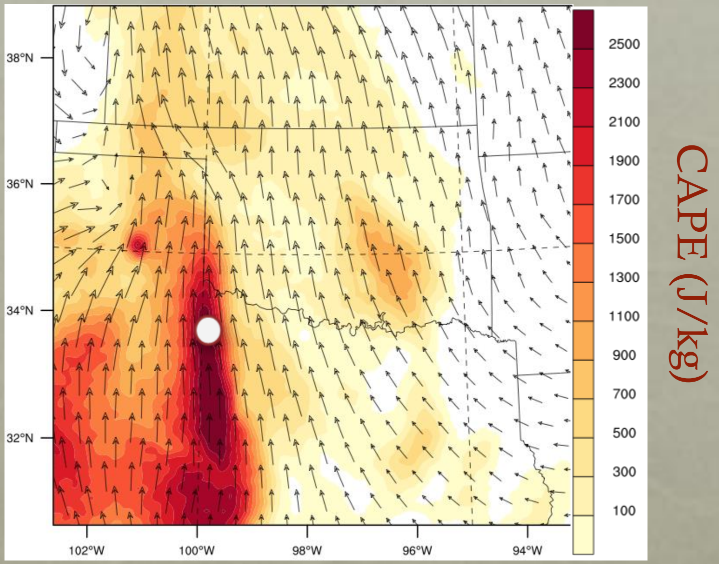

- Veering wind profile evident from bulk shear vectors and sounding (next slide)
- Southerly LLJ (18-21 m s^{-1}) develops – strengthens to 25 m s^{-1} and becomes more SWrly with time
- Strong zonal gradient in CAPE & CIN evident along and east of LLJ

Sounding 0500 UTC

- Sounding from RAP model analysis data valid at 0500 UTC (plotted using the SHARPpy program)
- Corresponds to approximate location of low-level jet
- User-defined parcel lifted from 1 km AGL
- Most unstable parcel is ~850 m AGL

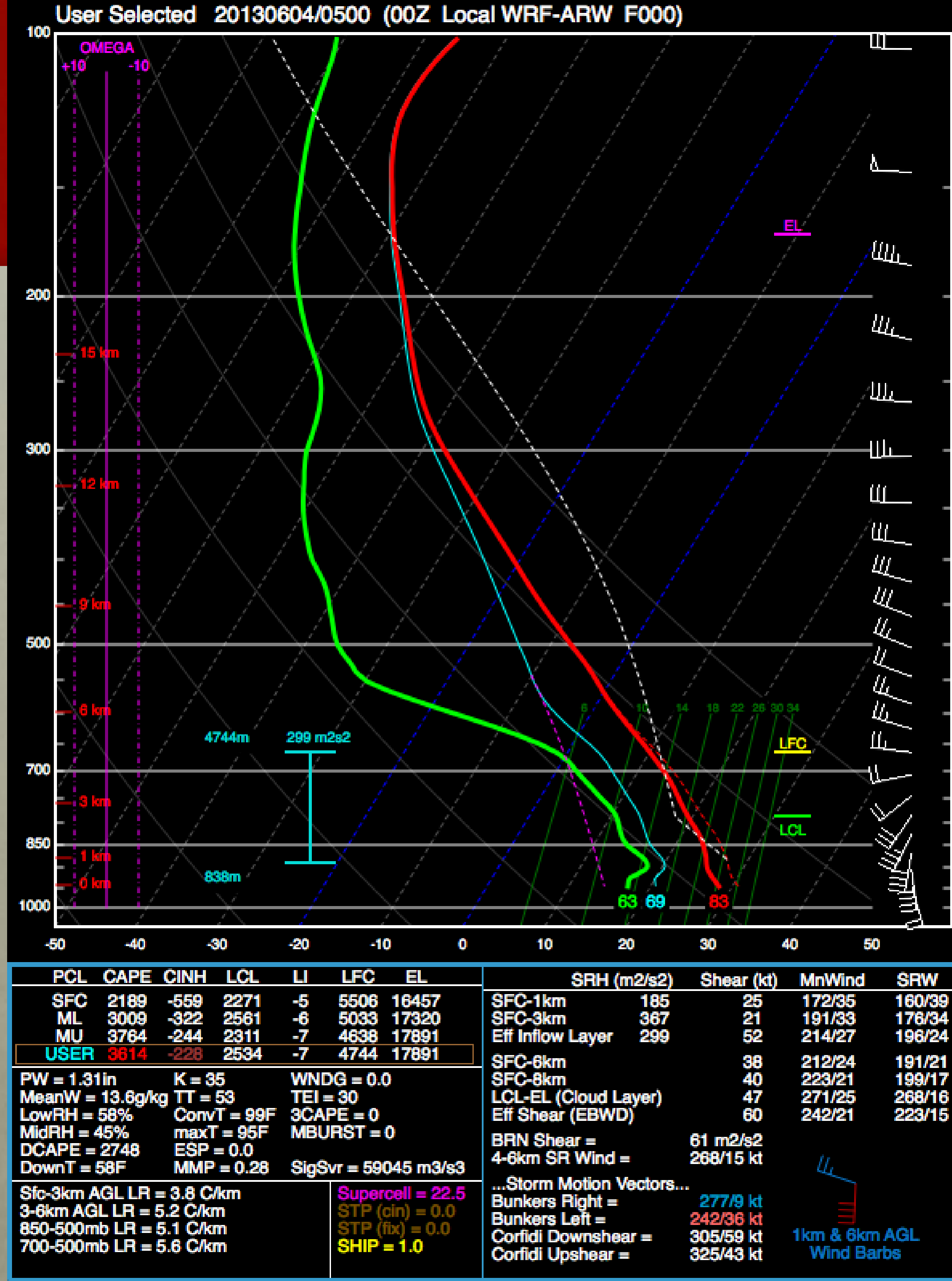

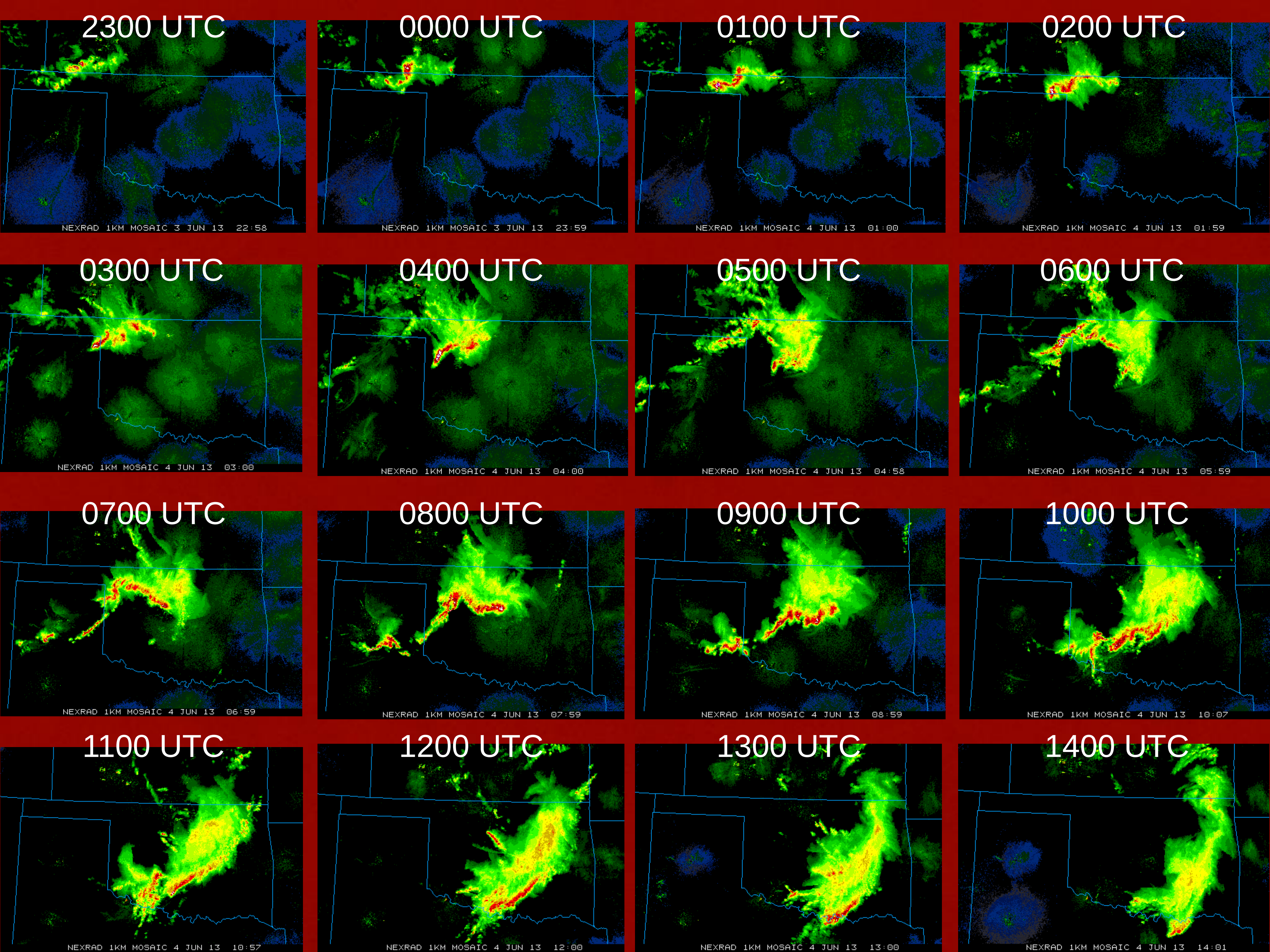
2300 UTC
NEXRAD 1KM MOSAIC 3 JUN 13 22:58
0000 UTC
NEXRAD 1KM MOSAIC 3 JUN 13 23:59
0100 UTC
NEXRAD 1KM MOSAIC 4 JUN 13 01:00
0200 UTC
NEXRAD 1KM MOSAIC 4 JUN 13 01:59
0300 UTC
NEXRAD 1KM MOSAIC 4 JUN 13 03:00
0400 UTC
NEXRAD 1KM MOSAIC 4 JUN 13 04:00
0500 UTC
NEXRAD 1KM MOSAIC 4 JUN 13 04:58
0600 UTC
NEXRAD 1KM MOSAIC 4 JUN 13 05:59
0700 UTC
NEXRAD 1KM MOSAIC 4 JUN 13 06:59
0800 UTC
NEXRAD 1KM MOSAIC 4 JUN 13 07:59
0900 UTC
NEXRAD 1KM MOSAIC 4 JUN 13 08:59
1000 UTC
NEXRAD 1KM MOSAIC 4 JUN 13 10:07
1100 UTC
NEXRAD 1KM MOSAIC 4 JUN 13 10:57
1200 UTC
NEXRAD 1KM MOSAIC 4 JUN 13 12:00
1300 UTC
NEXRAD 1KM MOSAIC 4 JUN 13 13:00
1400 UTC
NEXRAD 1KM MOSAIC 4 JUN 13 14:01

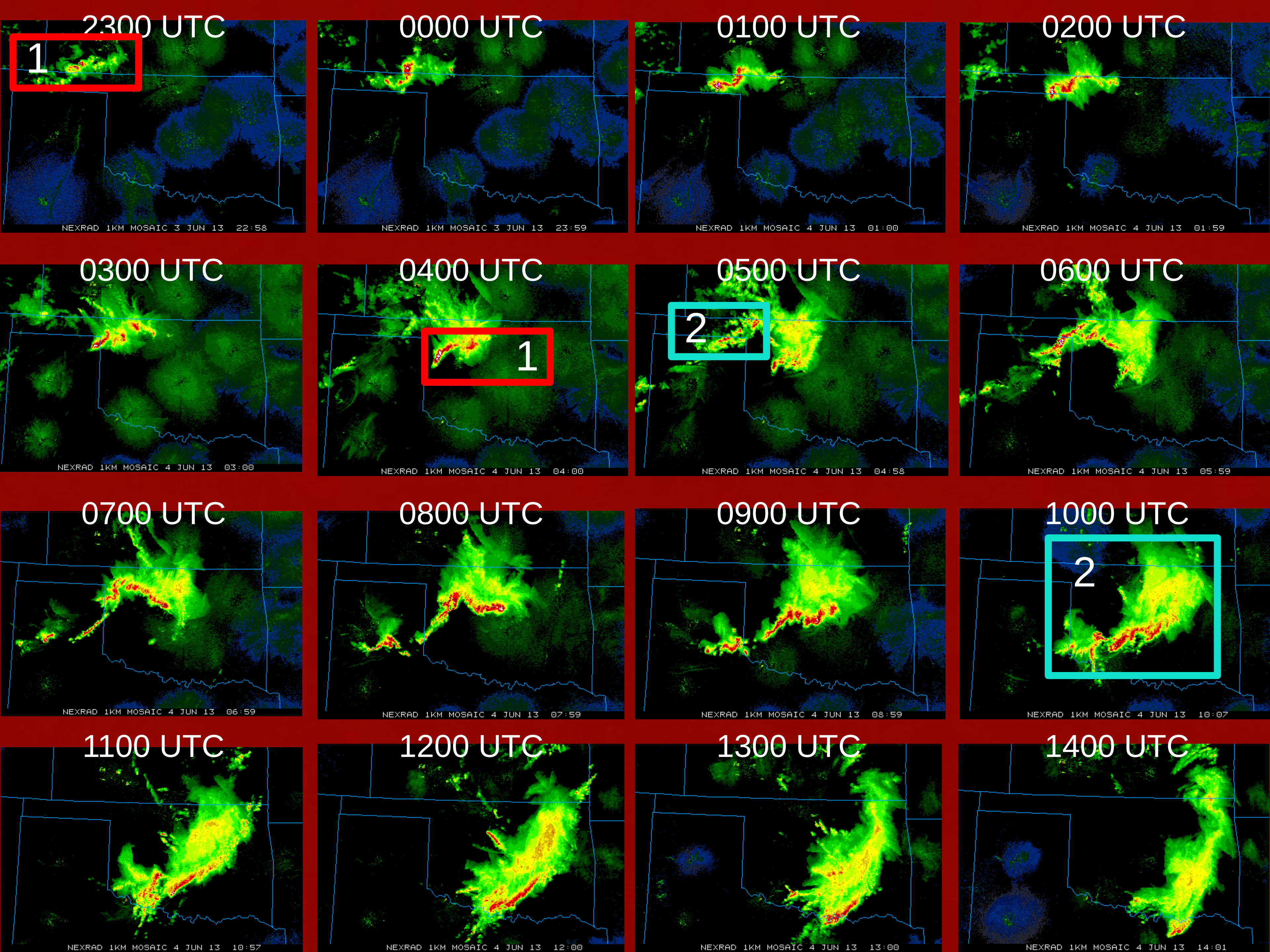
2300 UTC
1
NEXRAD 1KM MOSAIC 3 JUN 13 22:58
0000 UTC
NEXRAD 1KM MOSAIC 3 JUN 13 23:59
0100 UTC
NEXRAD 1KM MOSAIC 4 JUN 13 01:00
0200 UTC
NEXRAD 1KM MOSAIC 4 JUN 13 01:59
0300 UTC
NEXRAD 1KM MOSAIC 4 JUN 13 03:00
0400 UTC
1
NEXRAD 1KM MOSAIC 4 JUN 13 04:00
0500 UTC
2
NEXRAD 1KM MOSAIC 4 JUN 13 04:58
0600 UTC
NEXRAD 1KM MOSAIC 4 JUN 13 05:59
0700 UTC
NEXRAD 1KM MOSAIC 4 JUN 13 06:59
0800 UTC
NEXRAD 1KM MOSAIC 4 JUN 13 07:59
0900 UTC
NEXRAD 1KM MOSAIC 4 JUN 13 08:59
1000 UTC
2
NEXRAD 1KM MOSAIC 4 JUN 13 10:07
1100 UTC
NEXRAD 1KM MOSAIC 4 JUN 13 10:57
1200 UTC
NEXRAD 1KM MOSAIC 4 JUN 13 12:00
1300 UTC
NEXRAD 1KM MOSAIC 4 JUN 13 13:00
1400 UTC
NEXRAD 1KM MOSAIC 4 JUN 13 14:01

Observed Bores

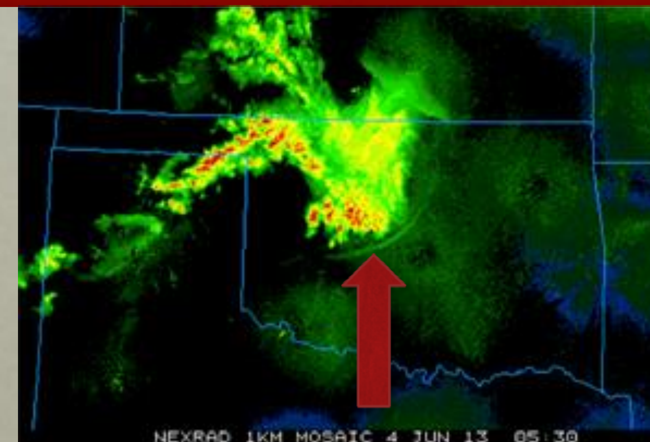

- First Bore: ~0500 – 0700 UTC
  - General lack of clouds, low liquid water paths
  - Reliable temperature and humidity observations obtained by the MP-3000A microwave radiometer on the roof of the National Weather Center in Norman, OK (Castleberry 2014)
- Second Bore: ~1000 UTC – dissipation of system
  - Close proximity of bore to convection, high liquid water paths
  - Accurate temperature and humidity observations unattainable (Castleberry 2014)

First Bore Observations

- Joint presence of moistening and cooling aloft suggestive of lifting by the bore
- Vertical displacements calculated using observed temperature changes and DALR
    - Max displacements approach 900 m from 1-3 km AGL with a net displacement of ~400 m after bore passage

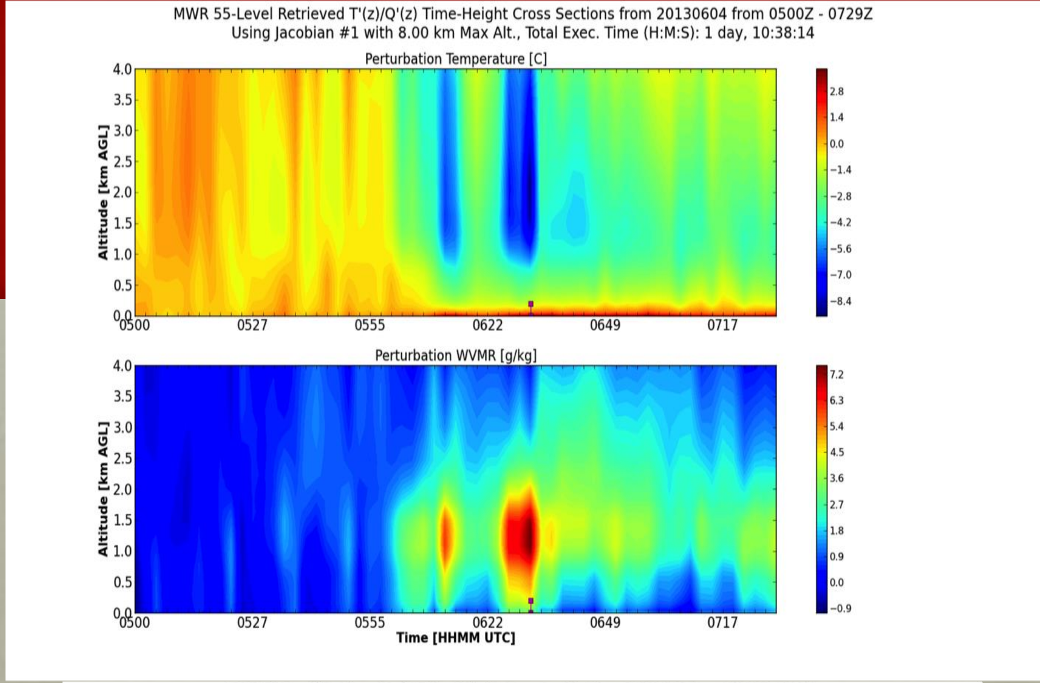

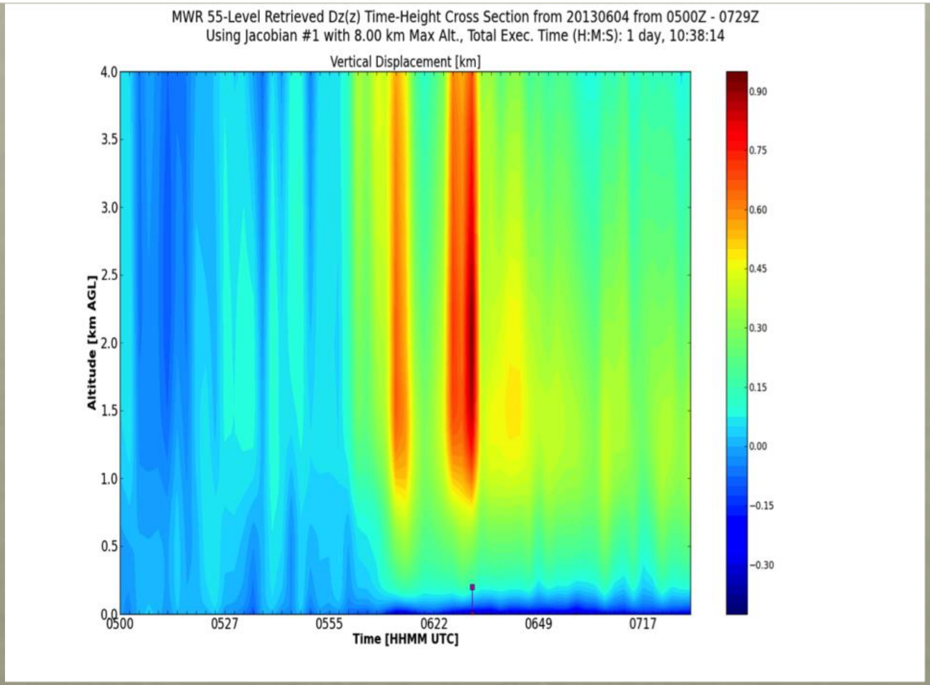

Figures courtesy of Stephen Castleberry

Model Configuration

- WRF-ARW Model Version 3.6.1
- 22 hour simulation: 1800 UTC June 3 to 1600 UTC June 4
- 3 Domains, Two Way Nesting
  - 100 vertical levels*
    - Added 10 eta levels below 1500 m
      - Vertical grid spacing is ~65 m
- Hourly initial and lateral boundary conditions
  - RAP atmospheric data
  - Noah LSM soil data

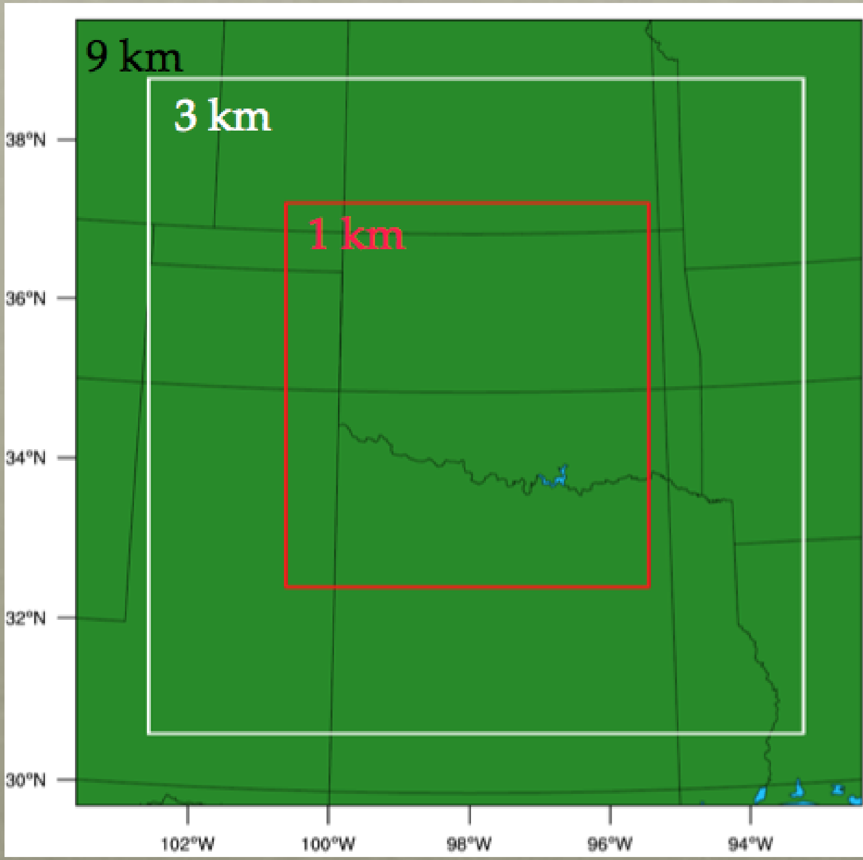

Parameterizations Control Simulation

Atmospheric Process	Parameterization Scheme	Notes & Reference
Longwave radiation	RRTM	Mlawer et al. 1997
Shortwave radiation	New Goddard	Chou & Suarez 1999
Cloud microphysics	Morrison	Double moment scheme; Morrison et al. 2009
Land surface model	Noah	Ek et al. 2003
Cumulus parameterization	BMJ	**Used in 9-km outer domain only;** Janjić 1994
PBL/Surface-layer scheme	MYNN Level 2.5	Local mixing scheme; Nakanishi & Niino 2004

General Evolution

Observed Reflectivity (dBZ) | Model Reflectivity (dBZ) | 500 m Wind Speed (m s^{-1})

2300 UTC

0200 UTC

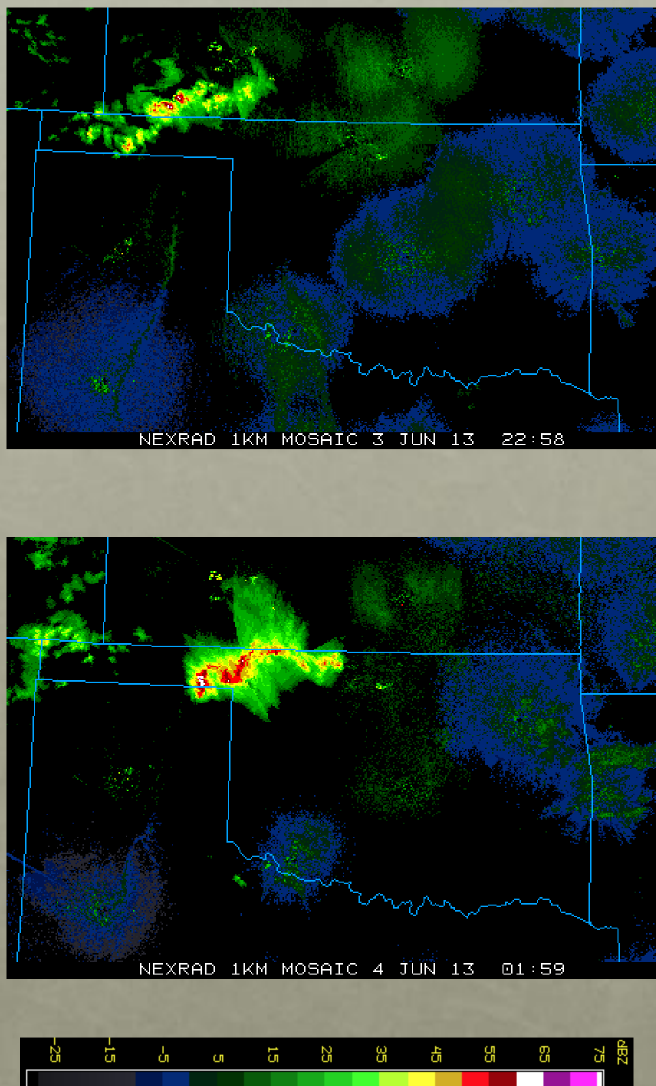

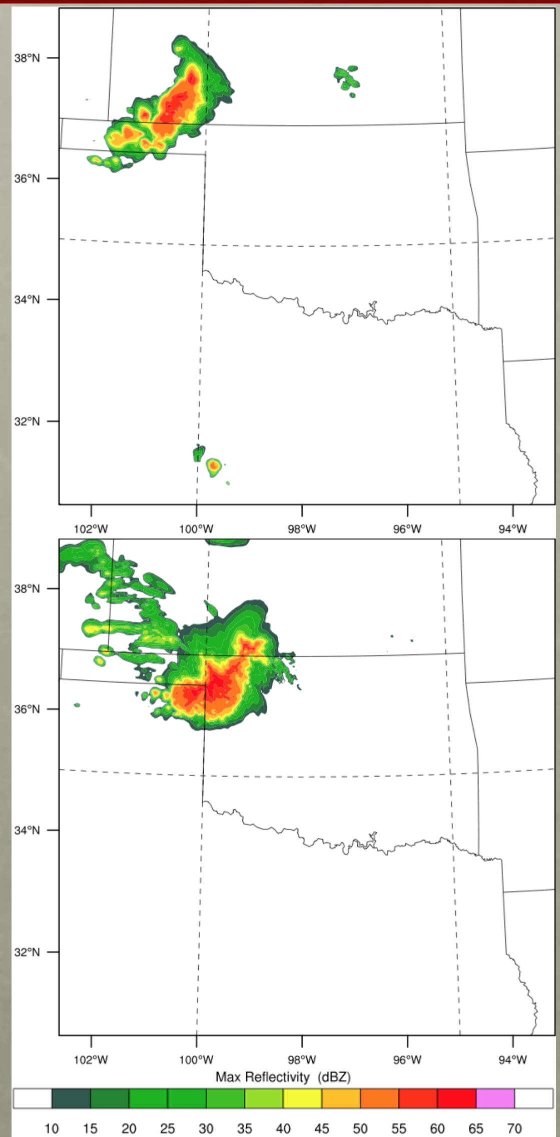

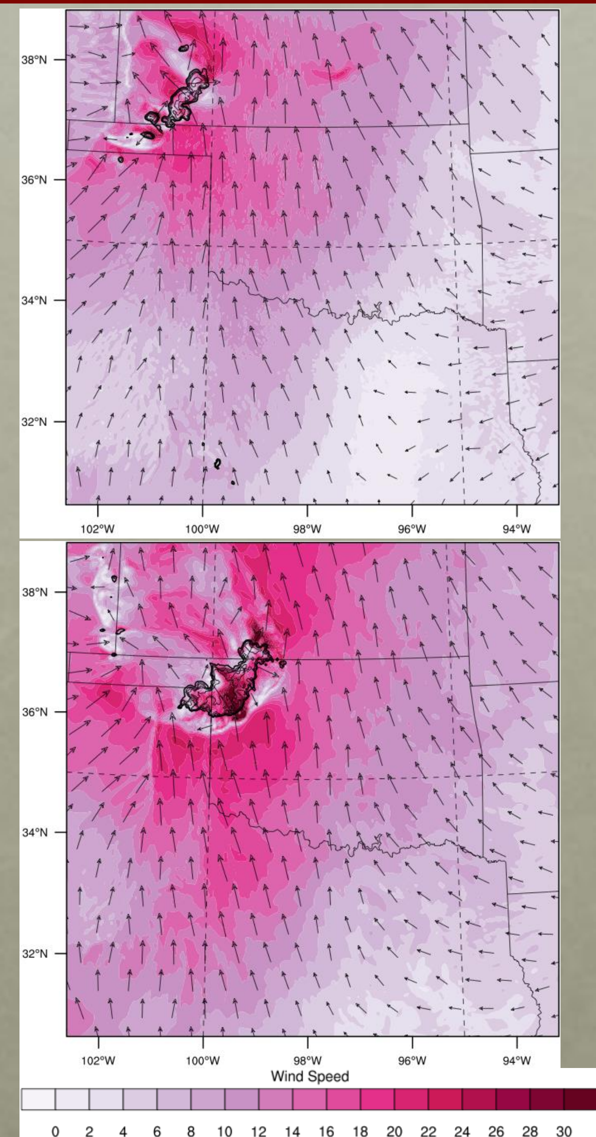

General Evolution

Observed Reflectivity (dBZ) | Model Reflectivity (dBZ) | 500 m Wind Speed (m s^{-1})

0530 UTC

0730 UTC

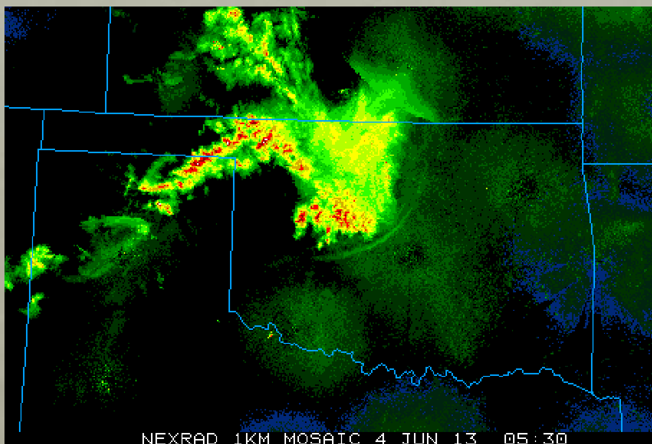

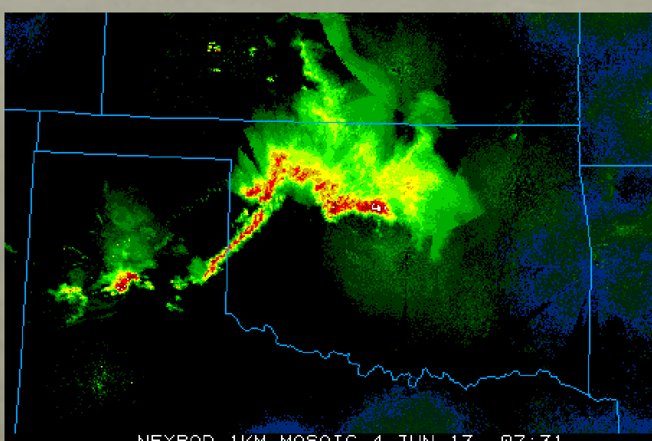

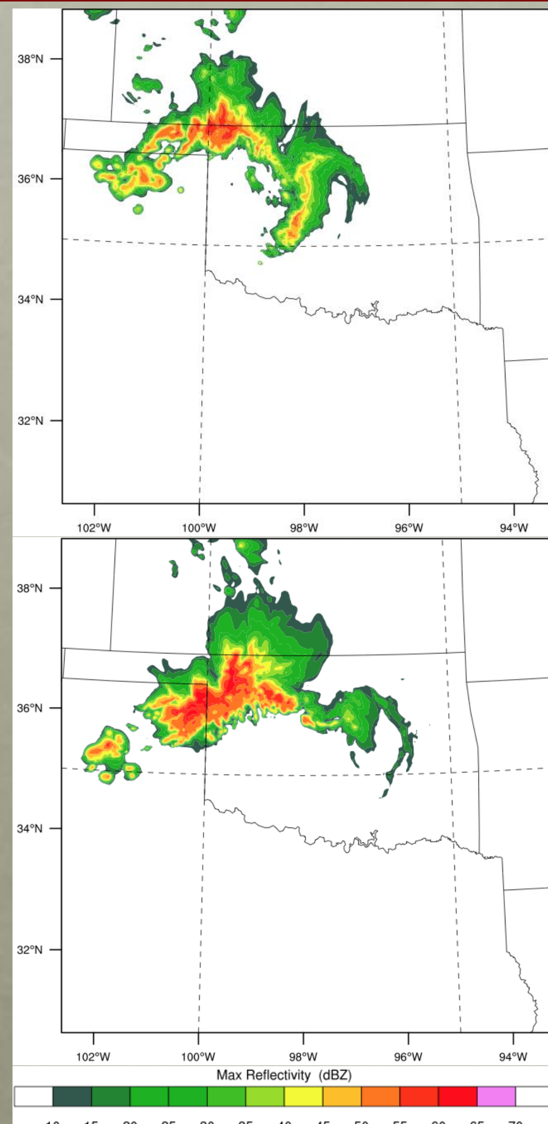

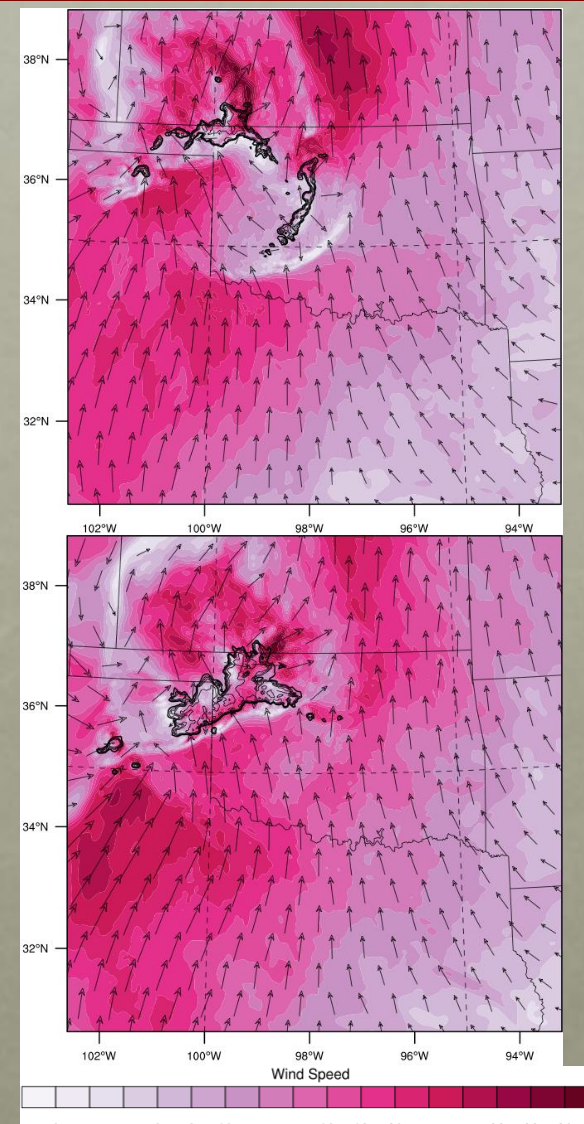

General Evolution

Observed Reflectivity (dBZ) | Model Reflectivity (dBZ) | 500 m Wind Speed (m s^{-1})

1000 UTC

1300 UTC

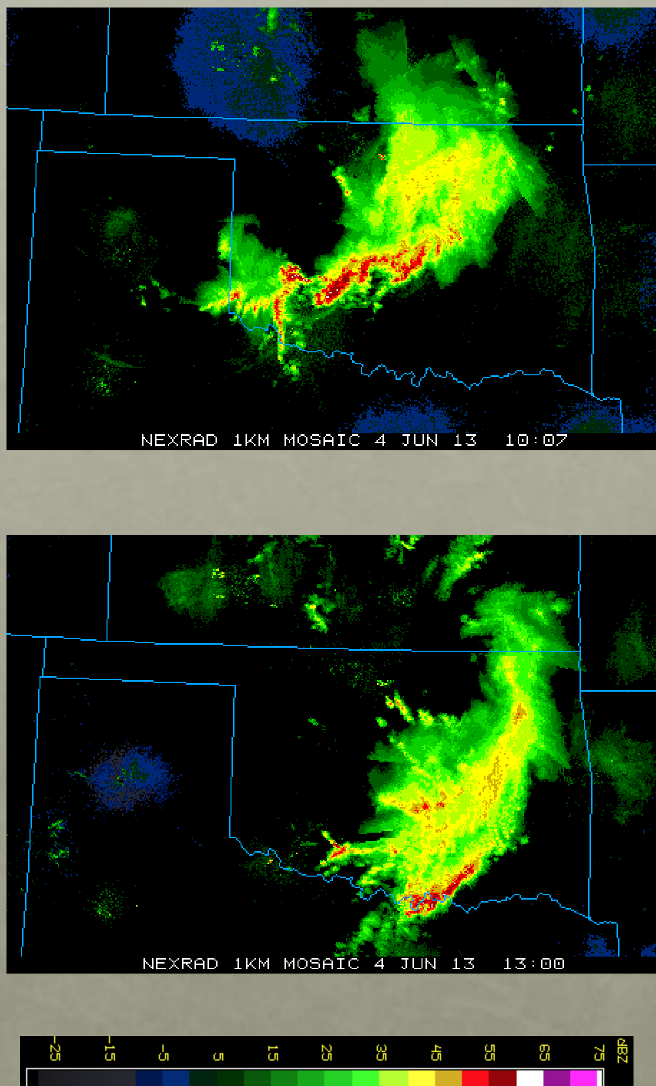

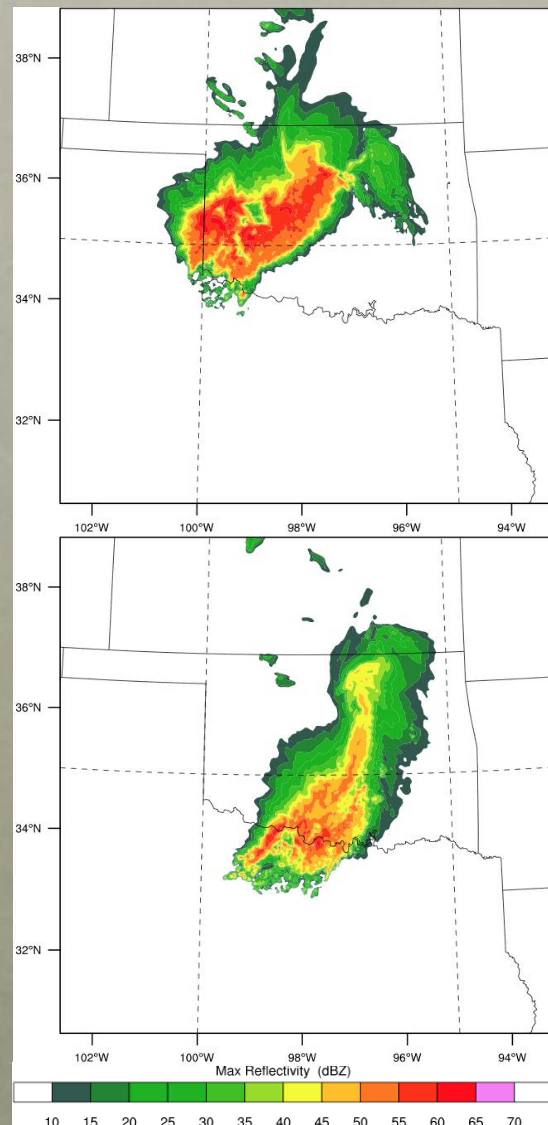

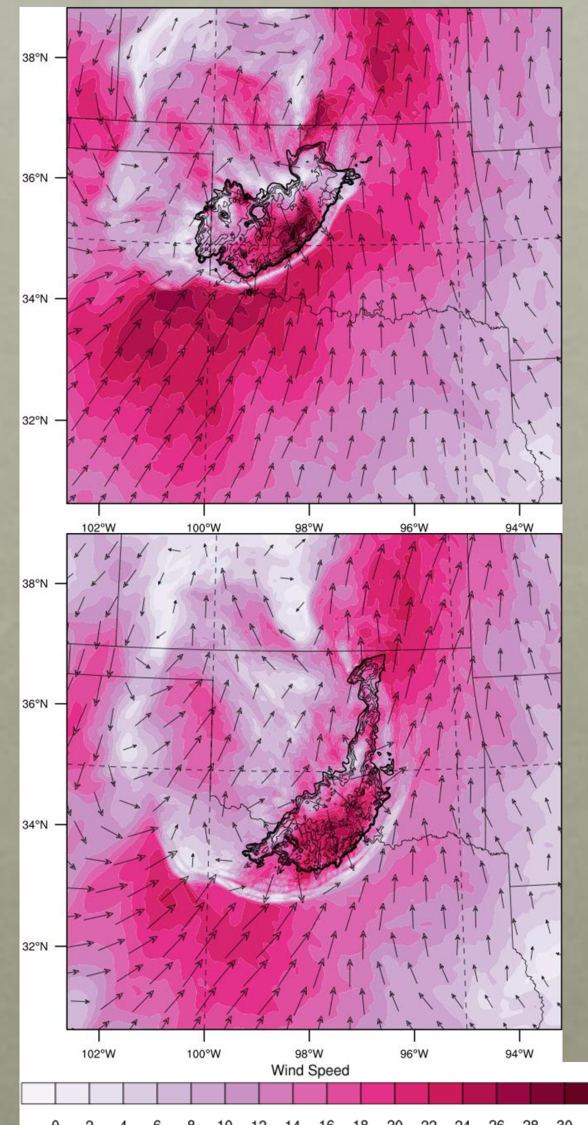

Sensitivity Tests

- Microphysics: WSM6, WDM6, NSSL 2-moment
  - Hail_opt run: allow Morrison scheme to utilize hail
- PBL: MYJ, YSU
- Remove 1-km inner domain
- # of Vertical Levels: 30, 53, 70, 100
- GFS run: Initial and lateral boundary conditions
- RAP data with analysis updates every 3 hours
- Damp_opt run: allow for damping at model top

Green indicates no significant change from control simulation

Outline

- Motivation/Background
- Brief Overview of 3-4 June 2013 MCS
- Model Configuration
- Control Simulation and Sensitivity Tests
- System Structure and Evolution
  - Advection by the LLJ
  - Surface vs. Elevated Cold Pool
  - Variation in structure around the cold pool
- Application of Theories to Variation in Structure
  - RKW framework
  - Wave theory framework
- Conclusions and Future Work

Questions to Answer

- How does the CAPE (surface-based and elevated) of the inflow evolve with time?
- What role does the nocturnal LLJ play in modifying the storm/its environment?
- Does the surface cold pool remain strong throughout the event?
- What causes the deep ascent to get parcels to their LFC?
- What types of outflows are produced and what role do these gravity currents/waves play in modifying the storm/its environment?

Evolution of CAPE & CIN in Surface & 1 km inflow regions

- Inflow Region: The region containing the air flowing into the storm

0700 CAPE at 1 km

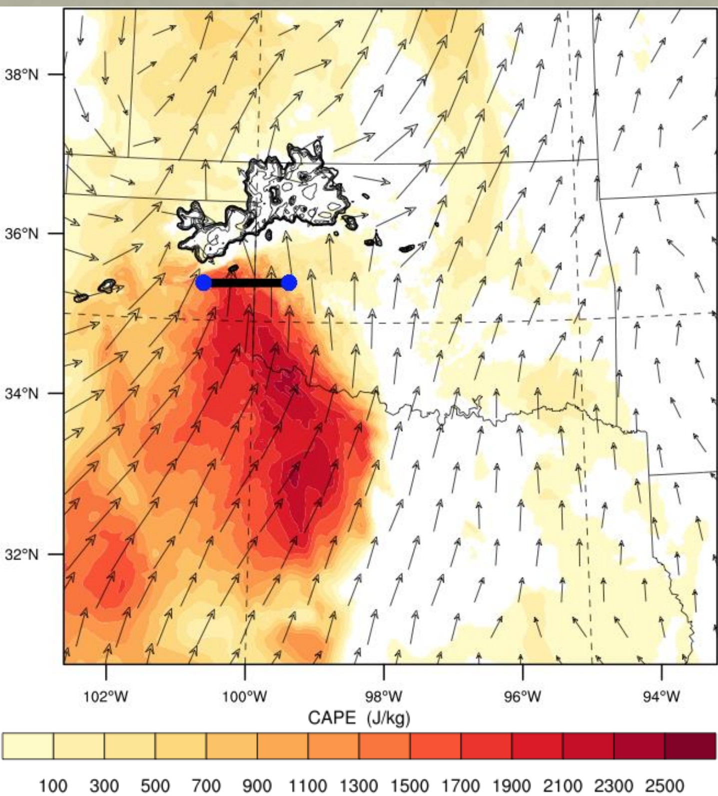

0700 CIN at 1 km

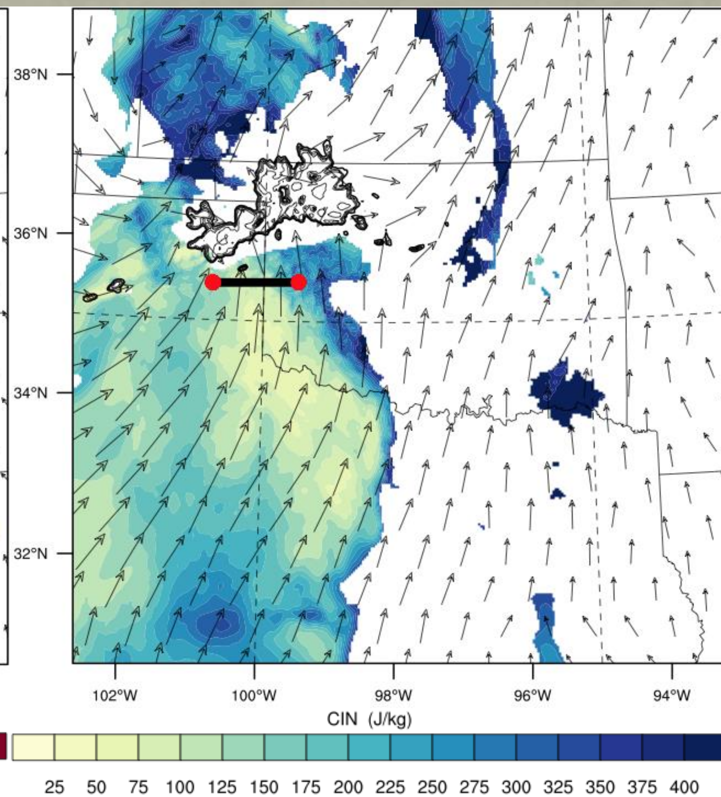

- ~130-150 km line drawn across inflow regions every 30 mins from 2300 to 1230 UTC
- CAPE & CIN calculated by averaging the values of ~9 points along each line (every ~15 km)

Evolution of CAPE & CIN in Surface & 1 km inflow regions

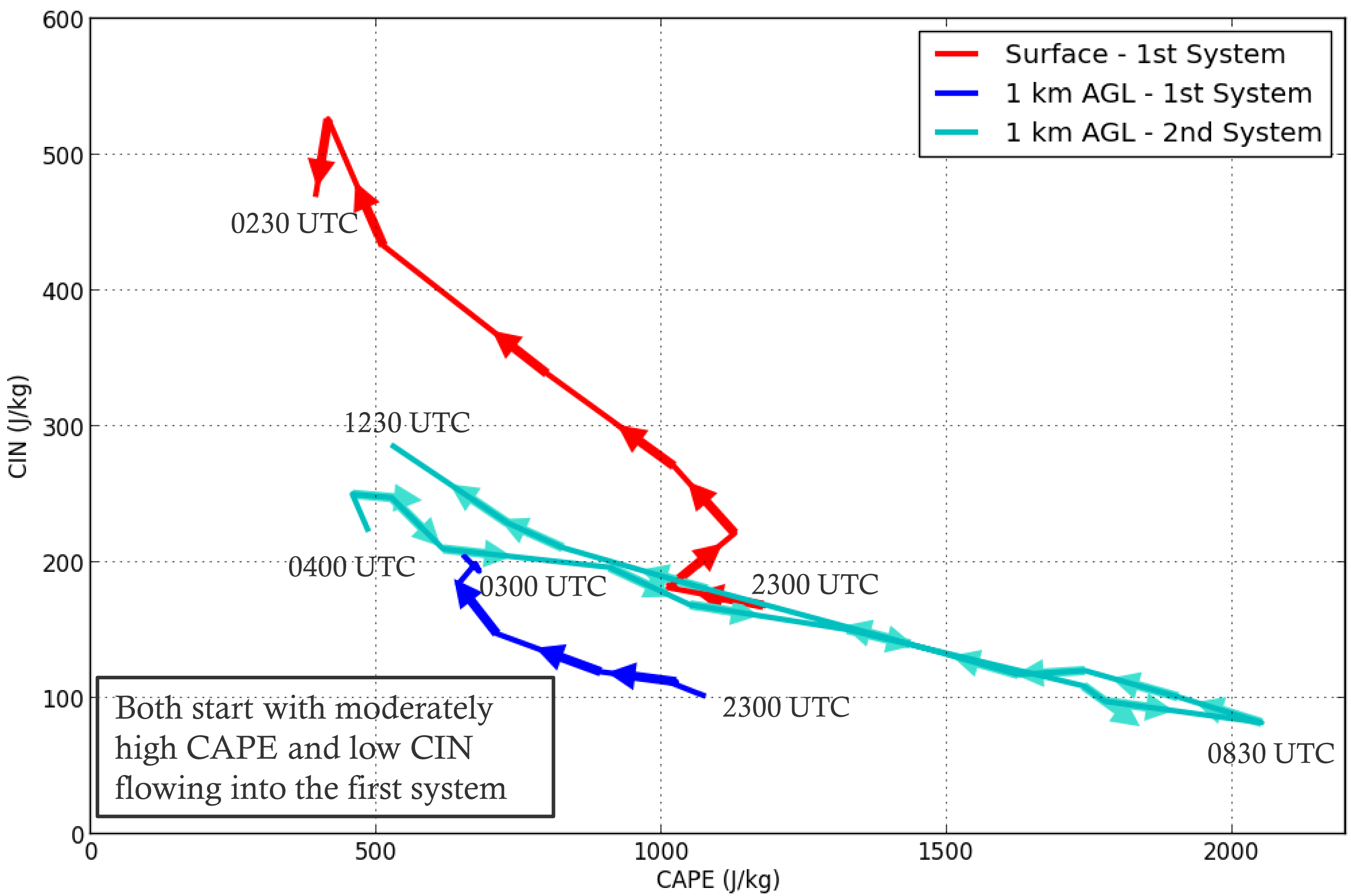

Evolution of CAPE & CIN in Surface & 1 km inflow regions

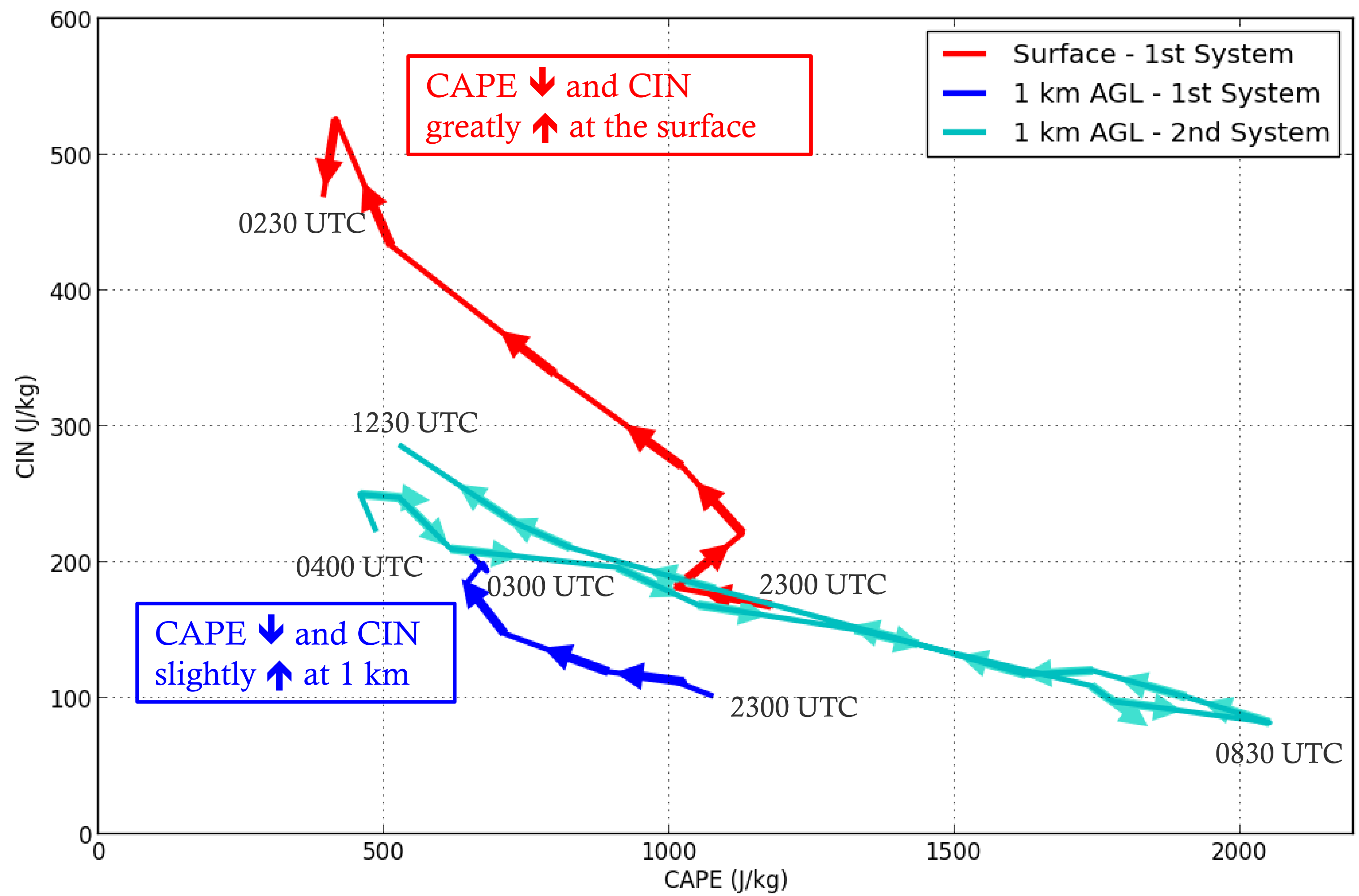

Evolution of CAPE & CIN in Surface & 1 km inflow regions

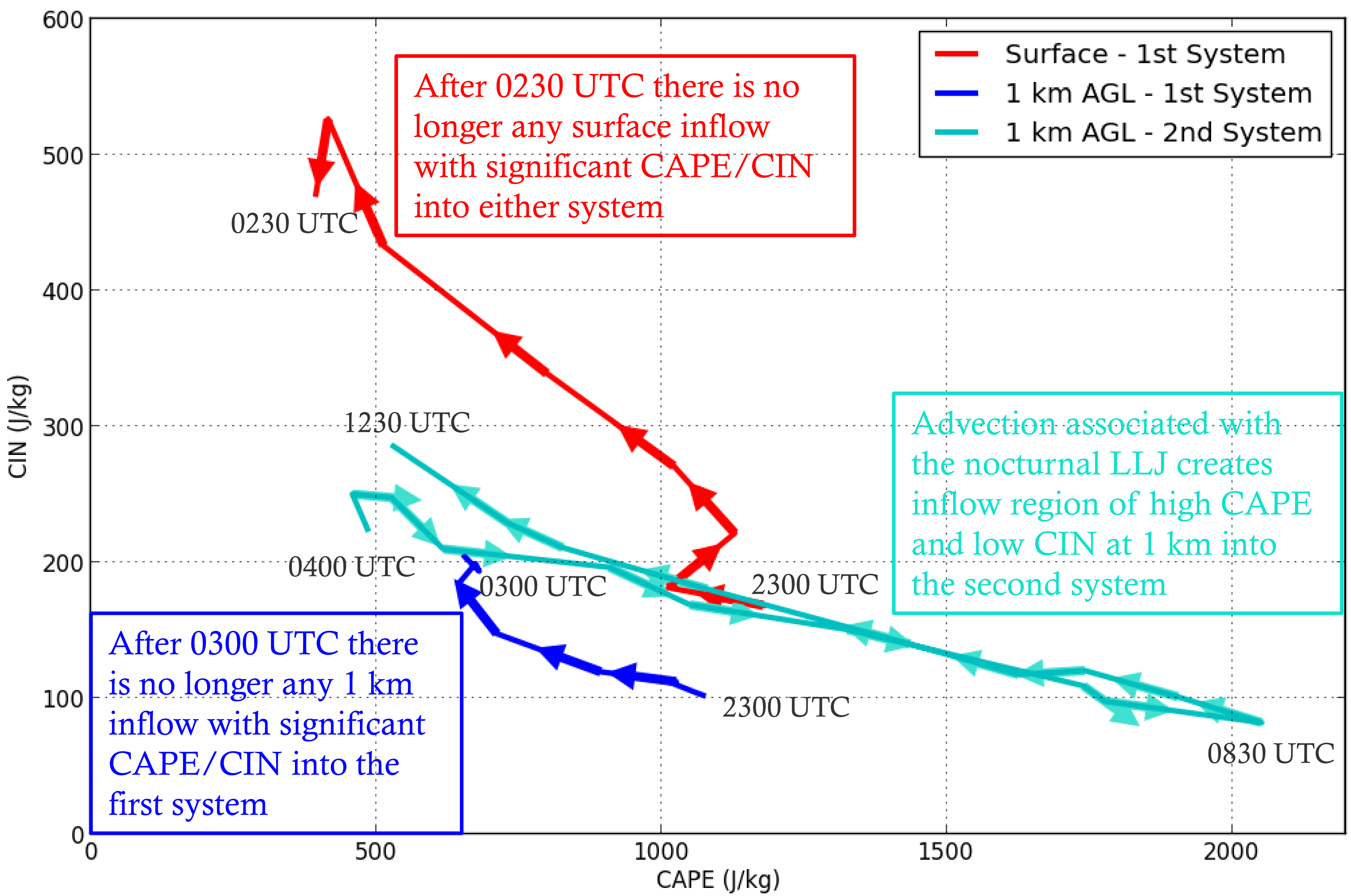

CAPE & Mixing Ratio at 1 km AGL

- South to north corridor of high CAPE values over western OK and the TX panhandle
- High CAPE correlated with high mixing ratios
- **Advection associated with the nocturnal LLJ brings moist, unstable air into the storm**

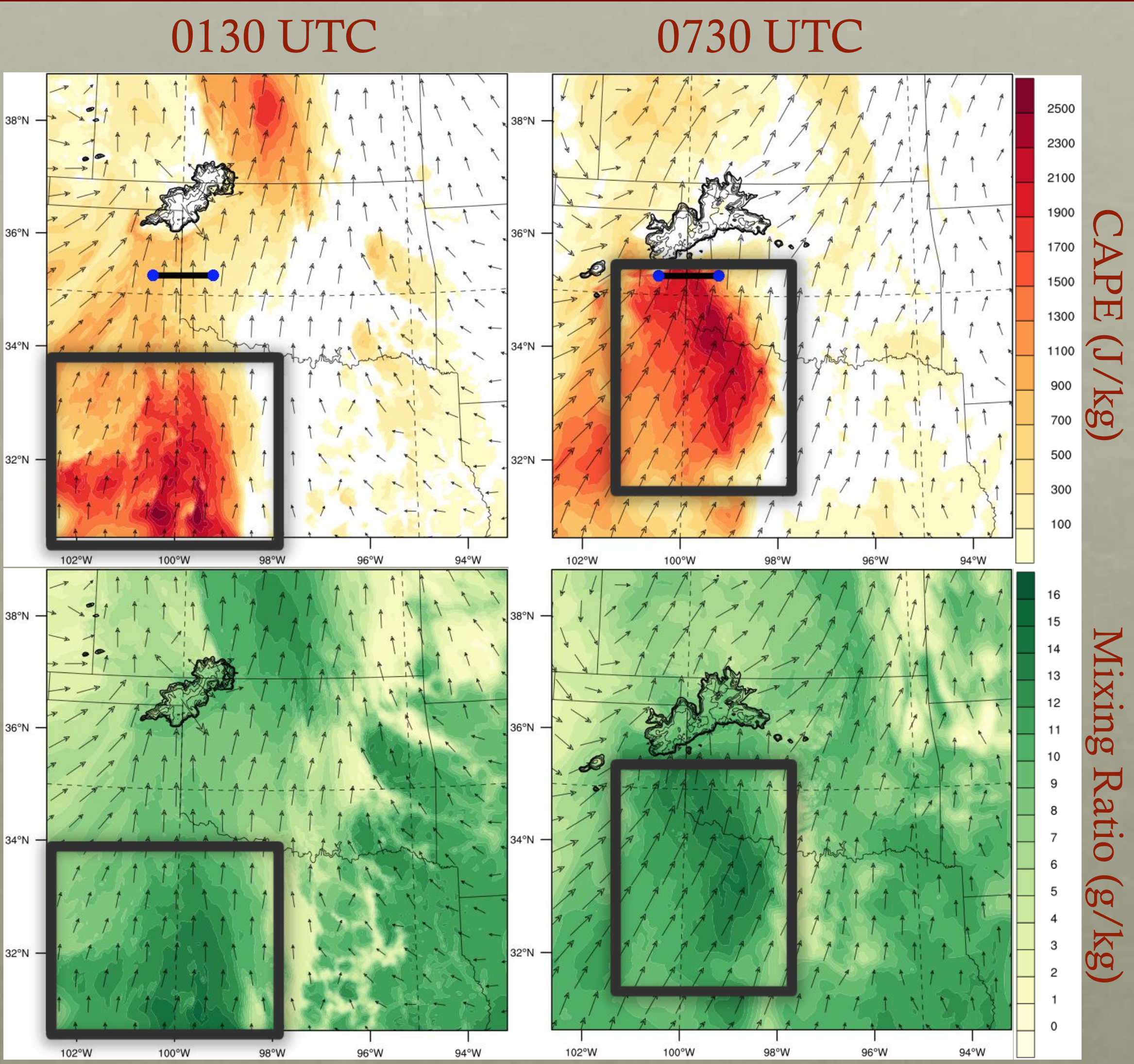

LLJ Advection 0400 to 0800 UTC

- 3-D trajectories constructed with VAPOR in 1-km domain using 5-min output from WRF
- During CI, inflowing air parcels primarily originate from SWrn part of the domain and are roughly 0.5-2 km AGL
- Corresponds to the location of the nocturnal LLJ

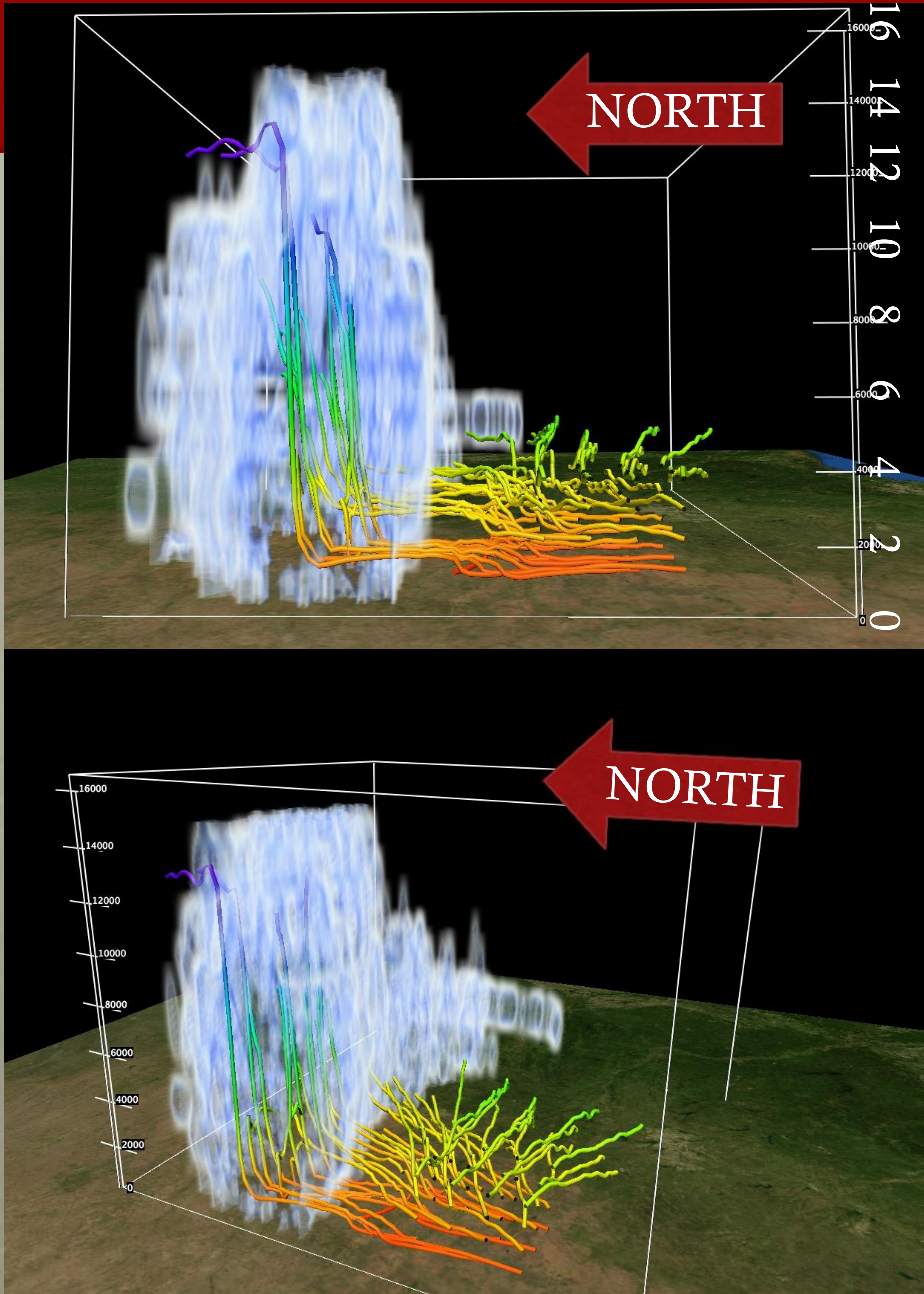

Evolution of Cold Pool Strength

- Cold Pool Strength: The temperature difference between the cold pool and the ambient air ahead of the storm
- ~85 km line drawn across cold pool and ~170 km line drawn across ambient air every 30 mins from 23 UTC 3 June to 1530 UTC 4 June
- Cold pool line located within 40 km behind the leading edge of the outflow and ambient air line located within 40 km ahead of the leading edge
- Temperatures calculated by averaging the values of ~5 points on cold pool line, ~9 points on ambient air line

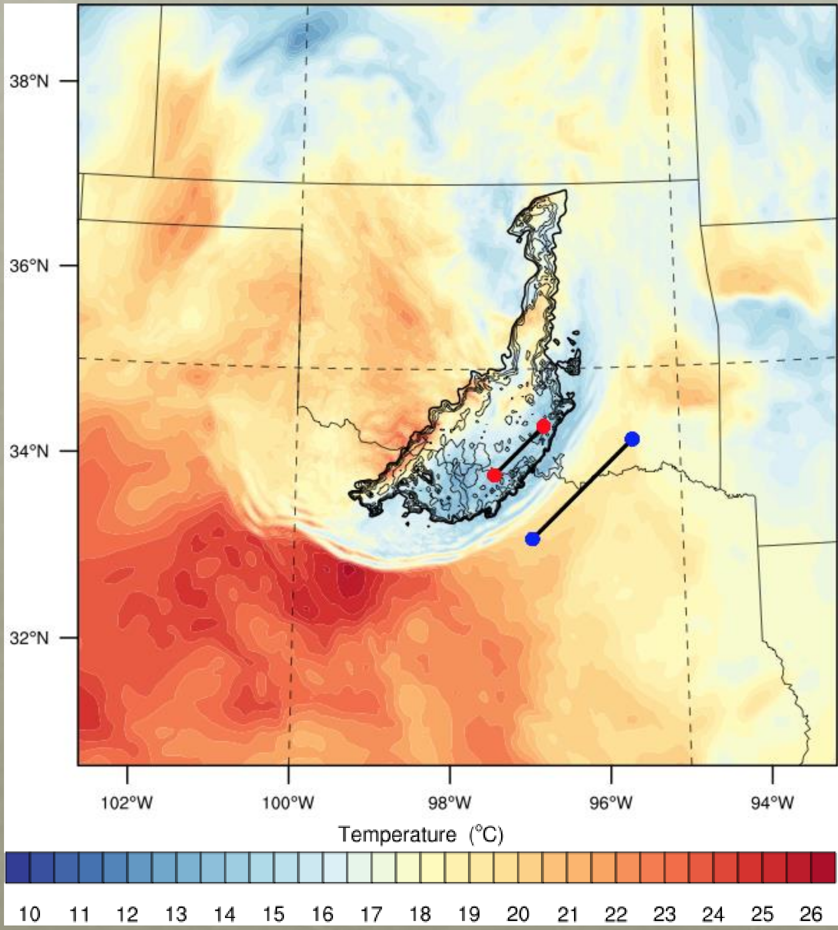

Evolution of Cold Pool Strength
Surface vs. 1 km AGL

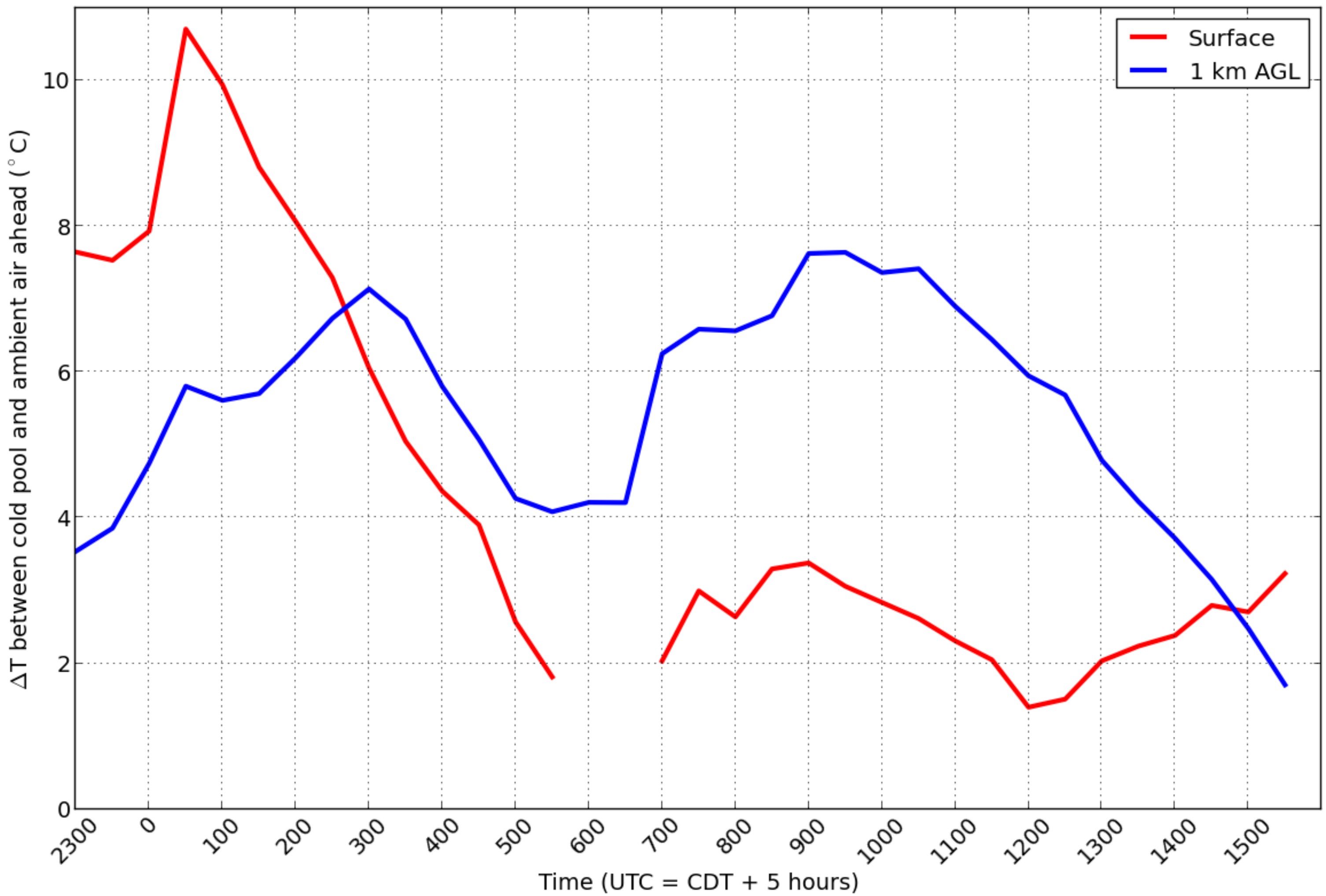

Evolution of Surface Cold Pool Strength WRF vs. Mesonet

Vertical Velocity & dBZ at 1 km AGL

- Structure of outflow changes with direction of propagation
- Convection primarily continues to the ESE
- Looked at 6 different propagation angles (21°, 0°, 344°, 330°, 315°, 293°)

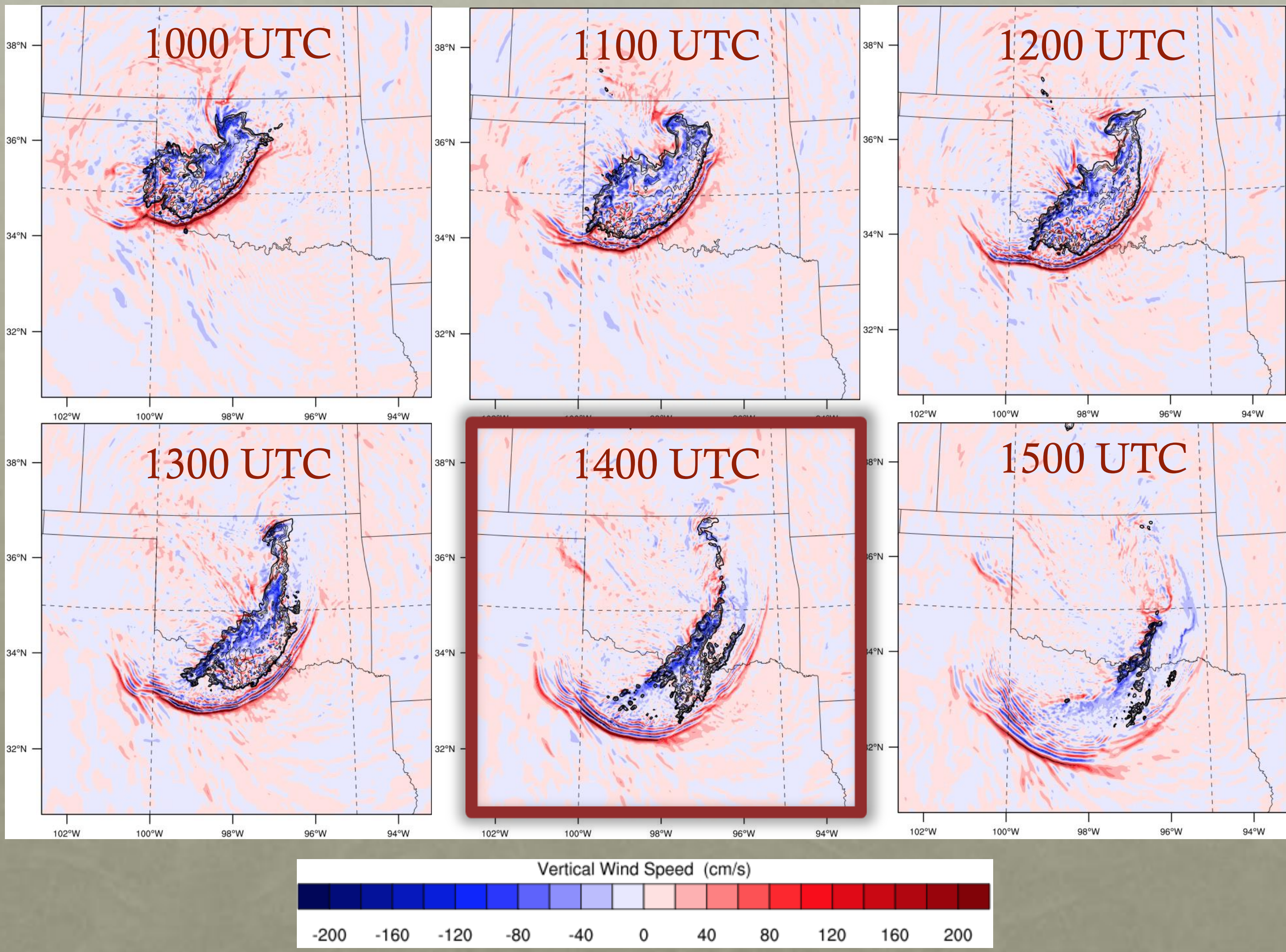

Vertical Velocity & dBZ at 1 km AGL

- Structure of outflow changes with direction of propagation
- Convection primarily continues to the ESE
- Looked at 6 different propagation angles (21°, 0°, 344°, 330°, 315°, 293°)

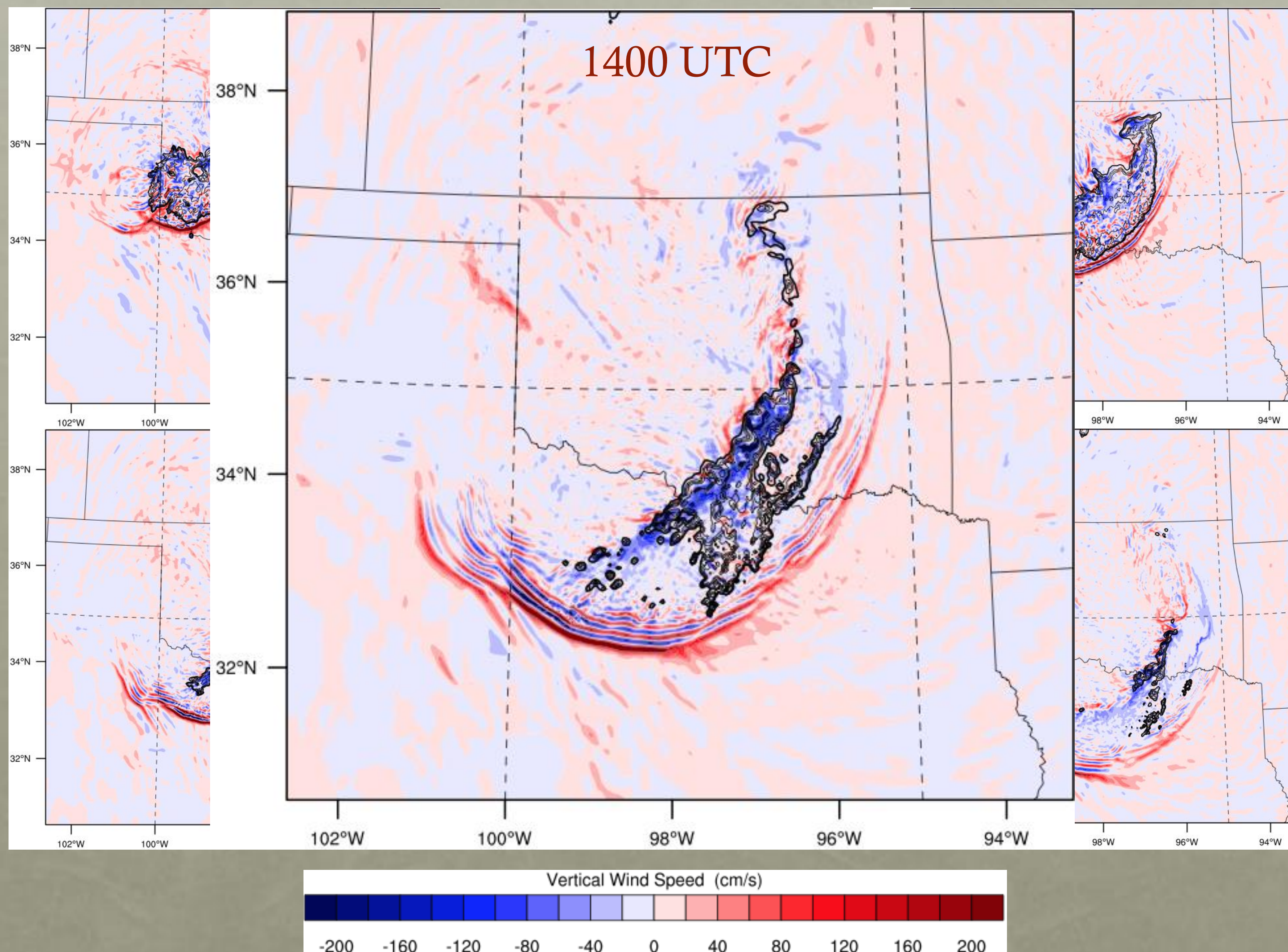

Elevated Buoyancy
1030 UTC

$$B \equiv g\left[\frac{\theta'}{\bar{\theta}} + 0.61(q_v - \bar{q}_v) - q_c - q_r\right]$$

0º Region (South End)

315º Region (SE End)

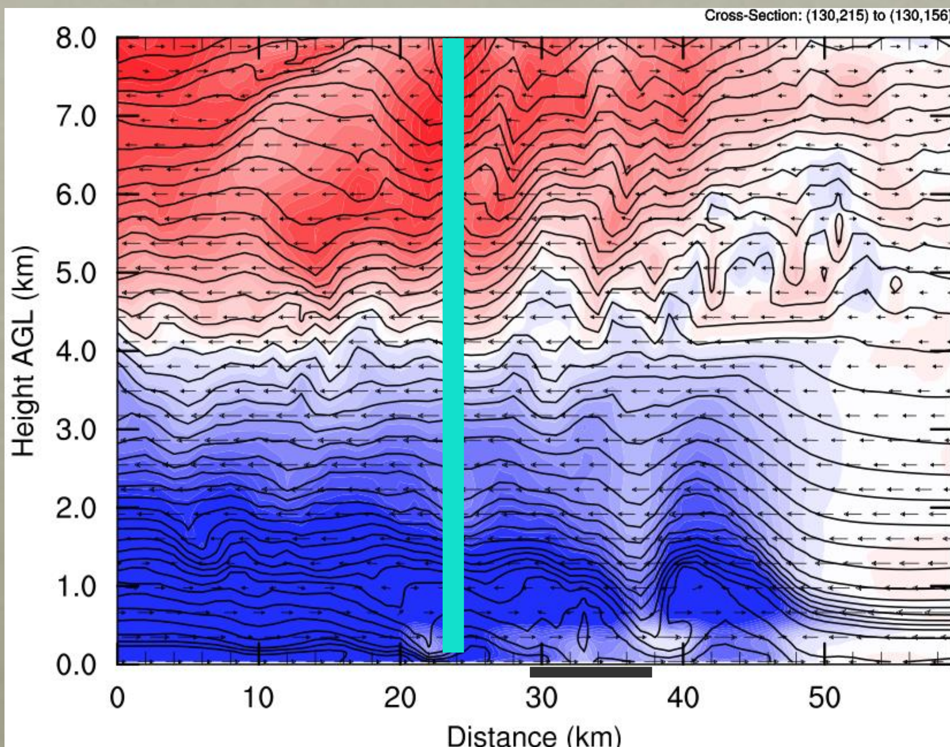

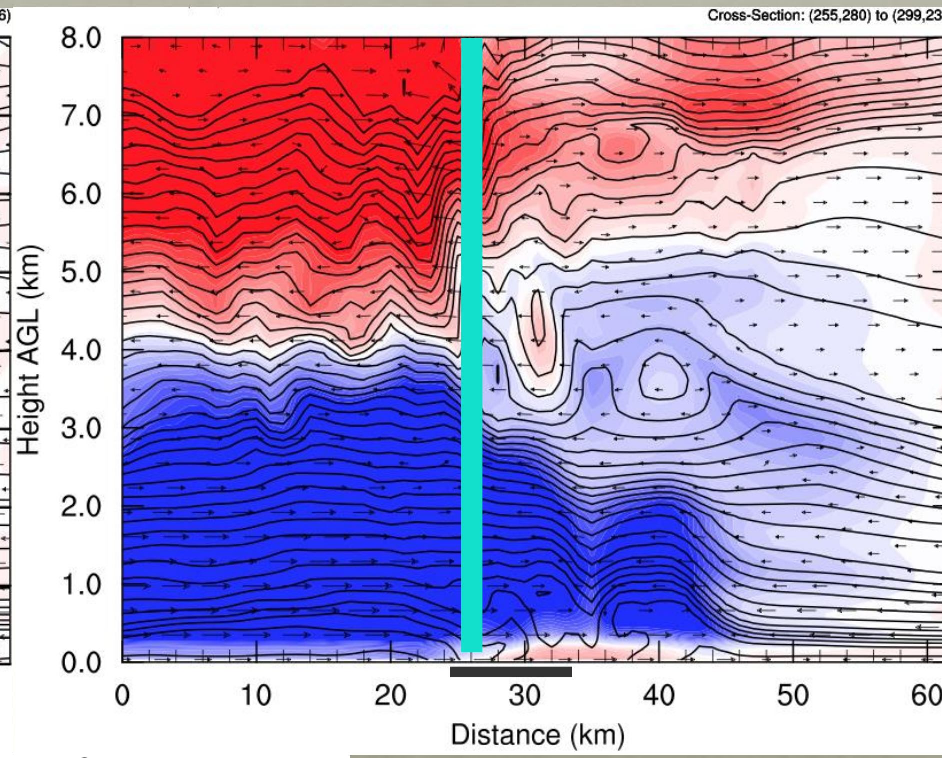

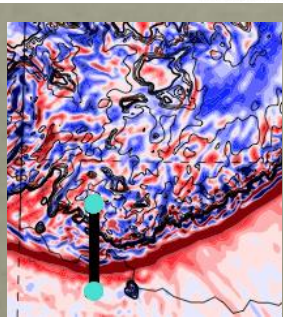

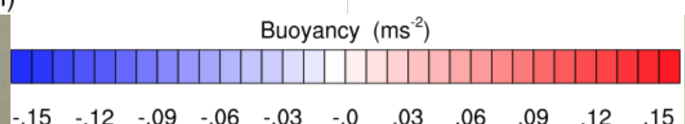

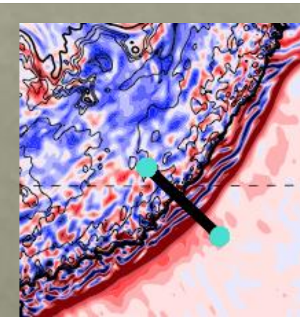

Vertical Velocity
1030 UTC

0º Region (South End)

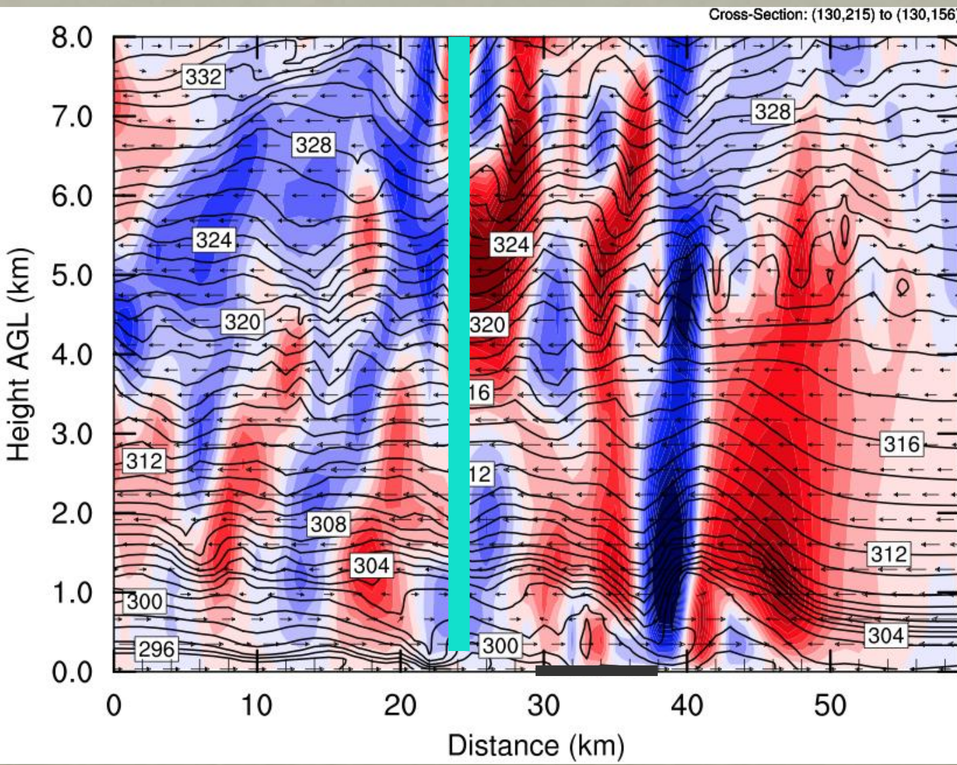

315º Region (SE End)

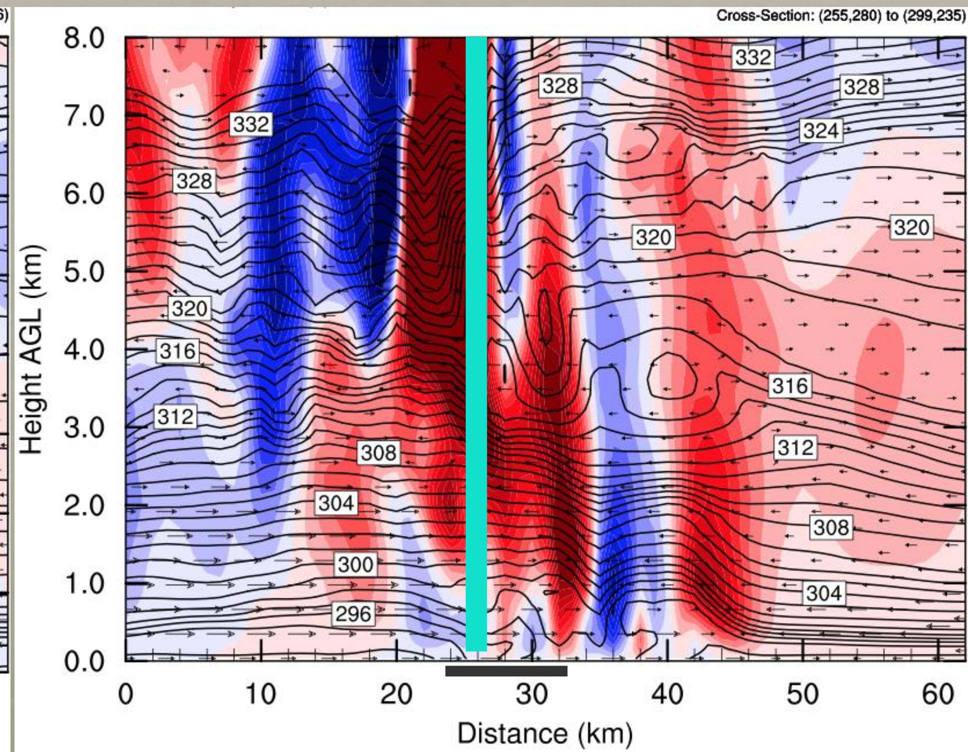

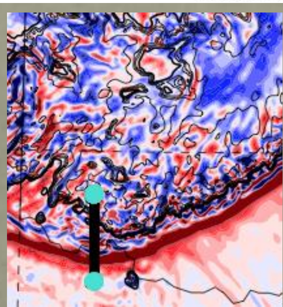

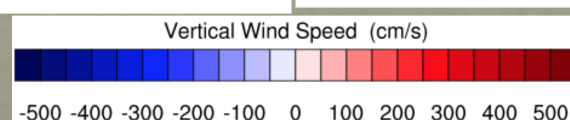

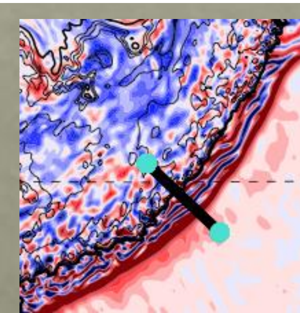

South End (0º)
1230, 1245, 1300, 1315 UTC

- Long-lived undular bore
- Below ~2 km: Upward motion is compensated by downward motion of a similar magnitude – solitary wave
- Bore lifting located primarily between ~2-4 km – well above the SBL (~300 m)
- Vertical motions trapped beneath ~5 km

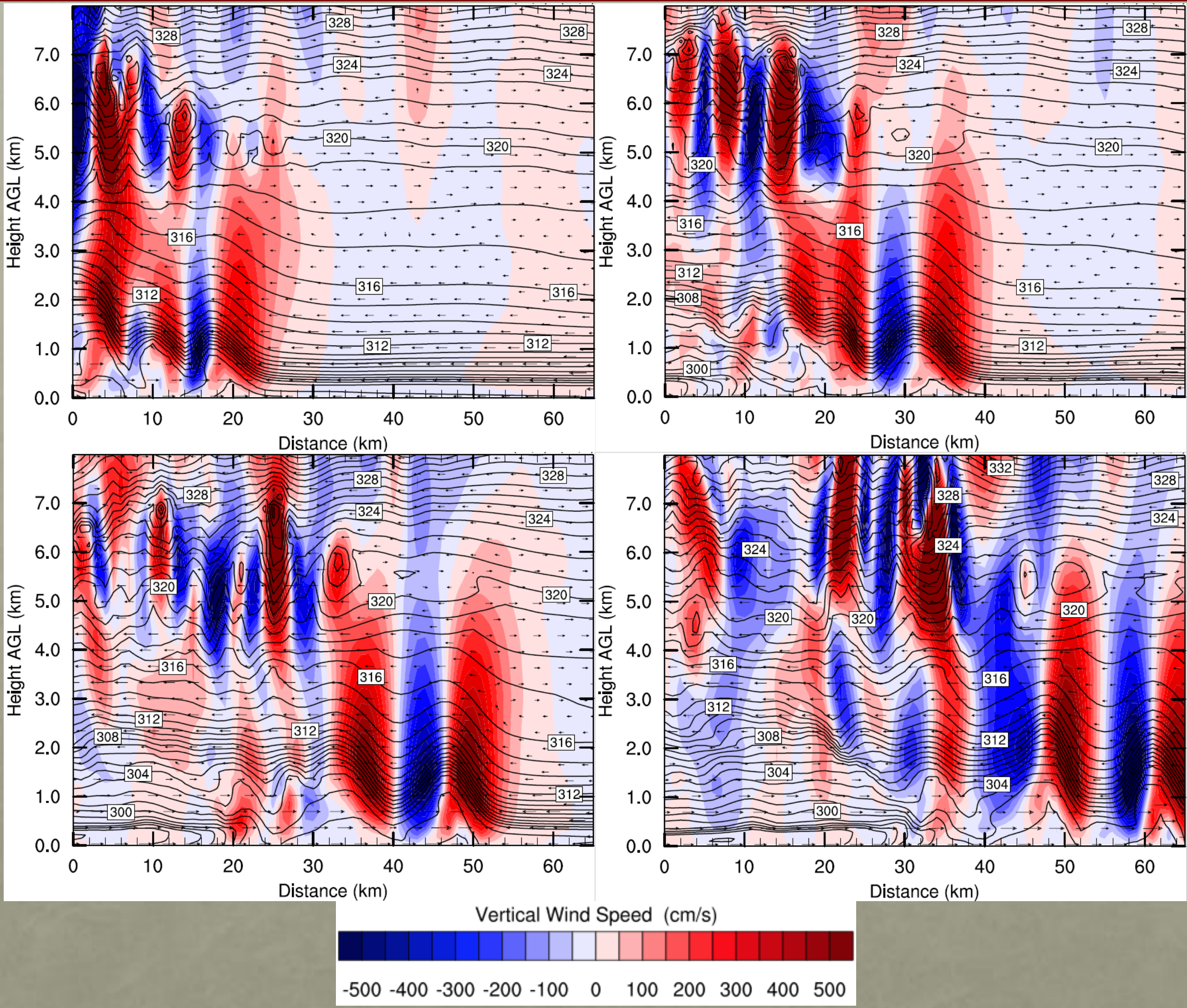

Southeast End (315º) 1230, 1245, 1300, 1315 UTC

- No long-lived undular bore, possible weak bore
- Regions of elevated lifting that expand/flatten with time (~2-5 km AGL)
  - Rarefaction waves (White and Helfrich 2012) and/or buoyancy bores (Mapes 1993)?
- Vertical motions not trapped beneath 5 km

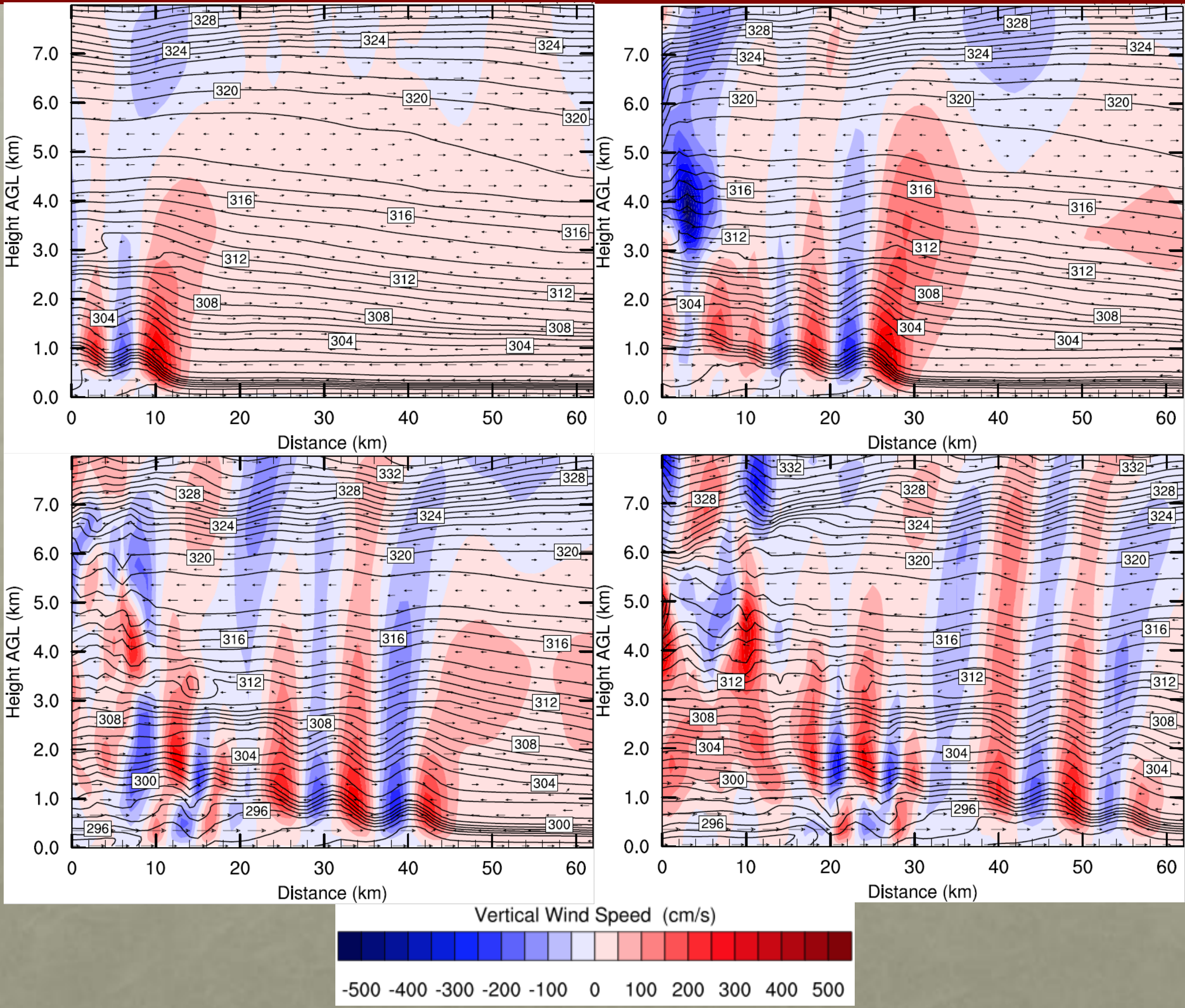

Findings on System Structure

- Highest CAPE and mixing ratios co-located with LLJ
- Cold pool transitions from being stronger at the surface to being stronger aloft
- Deep areas of negative buoyancy, esp. along active leading edge
- Positive buoyancy exists only above 4 km
- Lifting precedes the surface cold pool & area of active convection, similar to Fovell et al. (2006)
- Degree of lifting and type of waves varies strongly around the cold pool and extends well above the height of the LLJ and SBL
  - South End: Long-lived undular bore, was not limited to the low-level stable layer, but vertical motions trapped below ~5 km
  - Southeast End: Weaker wave features, regions of elevated lifting, and vertical motions not trapped below 5 km

Outline

- Motivation/Background
- Brief Overview of 3-4 June 2013 MCS
- Model Configuration
- Control Simulation and Sensitivity Tests
- System Structure and Evolution
  - Advection by the LLJ
  - Surface vs. Elevated Cold Pool
  - Variation in structure around the cold pool
- Application of Theories to Variation in Structure
  - RKW framework
  - Wave theory framework
- Conclusions and Future Work

Vorticity Balance (according to RKW theory)

- RKW Theory: An "optimal state" for convection (Rotunno et al. 1988)
- Negative horizontal vorticity produced baroclinically by the cold pool is exactly balanced by the positive horizontal vorticity associated with vertical wind shear in the environment
- + Vorticity produced in the environment by ambient vertical wind shear
    - Want dU/dz > 0
- Does not include the effects of a stable boundary layer, but French & Parker (2010) argue it holds aloft

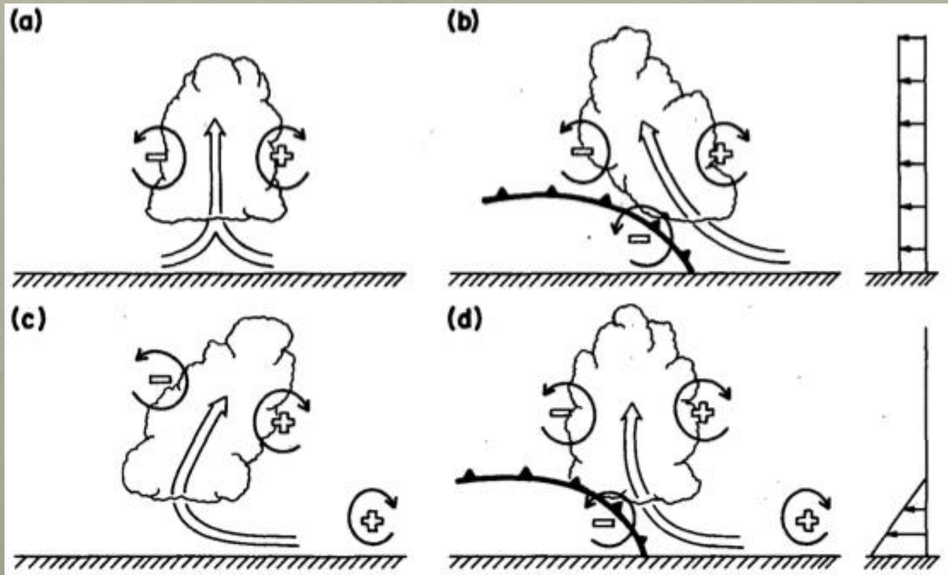

FIG. 18. Schematic diagram showing how a buoyant updraft may be influenced by wind shear and/or a cold pool. (a) With no shear and no cold pool, the axis of the updraft produced by the thermally created, symmetric vorticity distribution is vertical. (b) With a cold pool, the distribution is biased by the negative vorticity of the underlying cold pool and causes the updraft to lean upshear. (c) With shear, the distribution is biased toward positive vorticity and this causes the updraft to lean back over the cold pool. (d) With both a cold pool and shear, the two effects may negate each other, and allow an erect updraft.

Figure 18 from Rotunno et al. (1988)

Vertical Wind Shear 1000 UTC

- South End
  - LLJ contributes – vorticity below height of max wind
  - Effective shear layer with strongest + vorticity forcing located between ~0.6-1.25 km

- Southeast End
  - No LLJ but weak – vorticity forcing below 0.3 km
  - Deeper/stronger effective shear layer from ~0.35-1.25 km

- **More favorable vertical wind shear for deep ascent on the southeast end**

21° Region

315° Region

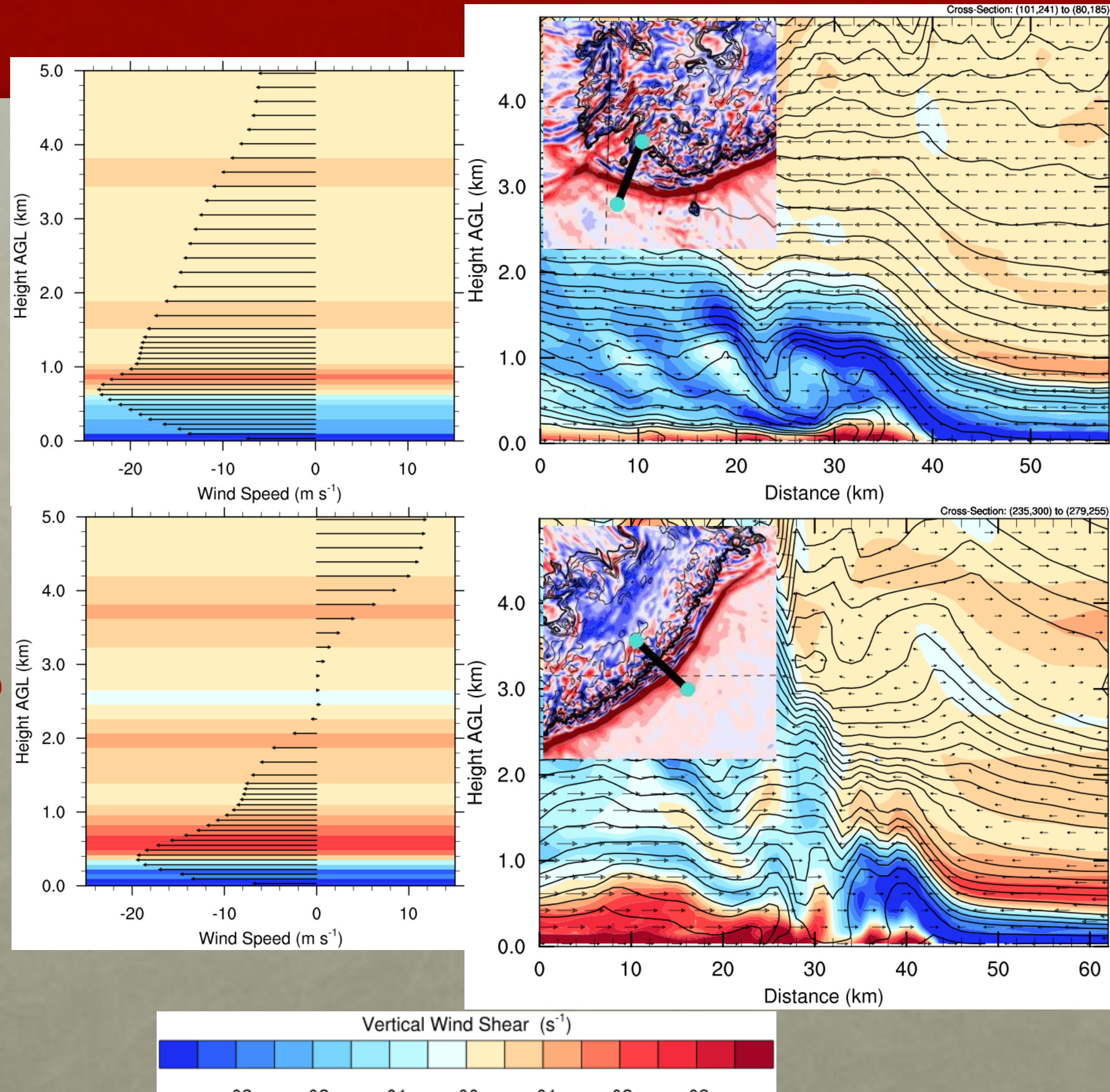

Horizontal Buoyancy Gradients

- -Vorticity produced baroclinically by the cold pool from horizontal gradients in buoyancy
  - Want dB/dx > 0 (dη/dt < 0)
  - Weisman (1992) used a similar approach to explain the internal structure of MCSs (rear-inflow jet, rear-to-front flow, etc.)

$$B \equiv g\left[\frac{\theta'}{\bar{\theta}} + 0.61(q_v - \bar{q}_v) - q_c - q_r\right]$$

2D Horizontal Vorticity Equation

$$\frac{d\eta}{dt} = -\frac{\partial B}{\partial x}$$

$$\eta = \frac{\partial u}{\partial z} - \frac{\partial w}{\partial x}$$

Horizontal Buoyancy Gradients 1030 UTC

- South End
  - Some positive B aloft
  - Alternating regions of -/+ vorticity forcing below 2 km, with – vorticity at the leading edge of the wave & the gravity current

- Southeast End
  - Significant + B aloft and more – B at low levels
  - More lift required to overcome negatively buoyant air
  - dB/dx reveals – vorticity forcing at leading edge of wave feature, which translates upward as it approaches gravity current

0º Region

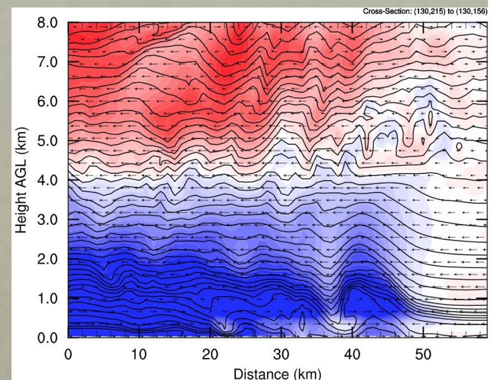

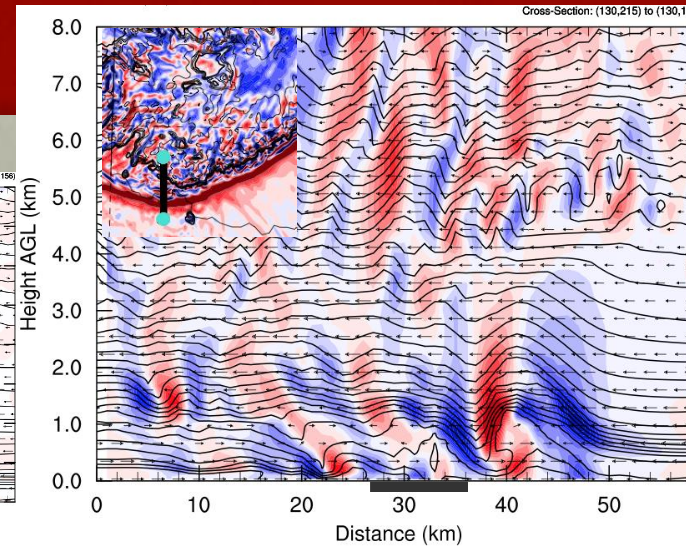

315º Region

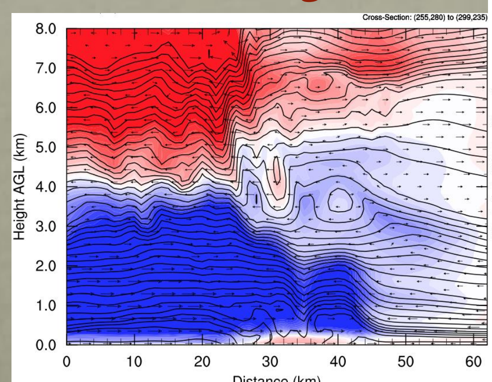

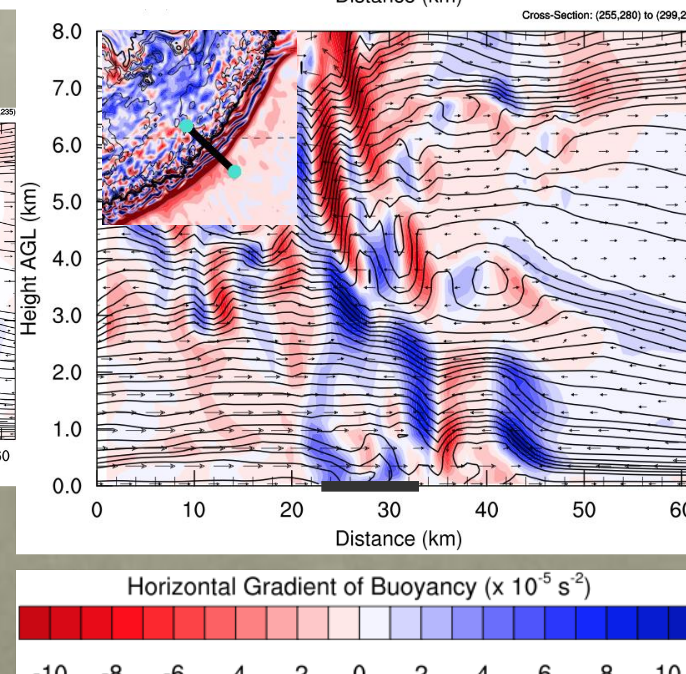

Vorticity Forcing Modification for Stable Boundary Layers

- New horizontal vorticity generation term ahead of & stronger than the cold pool due to lifting of stable air
- Term consistent with the surging forward of systems and high surface winds not concurrent with a cold pool
- What is causing this stable air to be lifted?
  - **Bores & Gravity Waves**

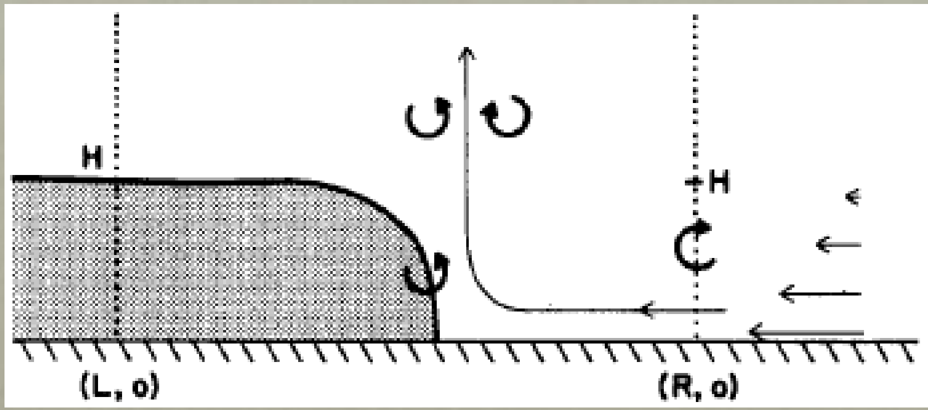

Figure 15a from Weisman (1992)

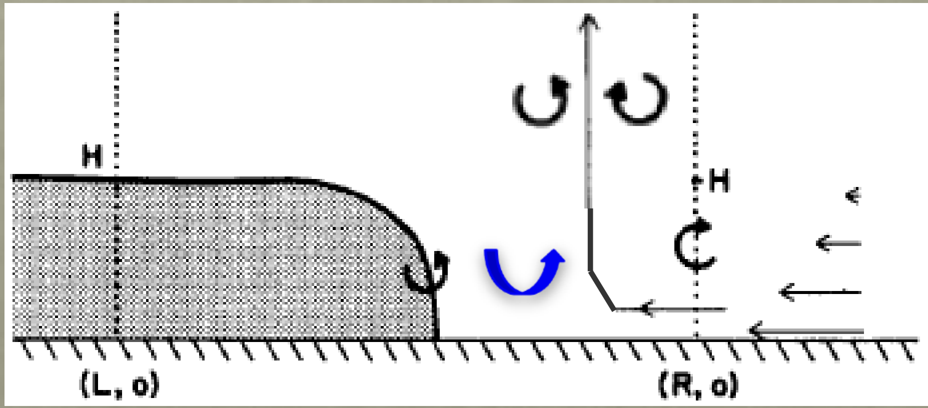

Hydraulic Theory

- 4 types of flow regimes can occur as a gravity current encounters a stable layer (Koch et al. 1991)
    - Supercritical flow
    - **Partially blocked**
    - **Completely blocked**
    - Subcritical flow

- Function of the nondimensional height ($D_o = d_o/h_o$) and Froude number (F)
    - d_o: depth of gravity current
    - h_o: inversion height

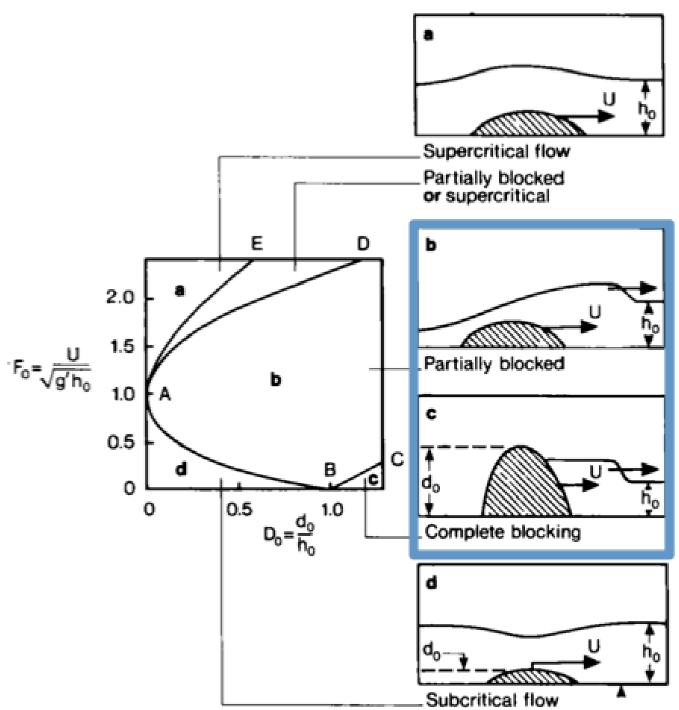

Must determine the flow regime. Bores will form in the partially or completely blocked regime.

Figure from Kevin Haghi (Originally from Rottman & Simpson 1989)

$$F = \frac{(U - C_{gc})}{C_{gw}} = \frac{(U - C_{gc})}{\sqrt{g\Delta\theta h_o/\theta_{vw}}}$$

Calculating Froude Number

$$F = \frac{(U - C_{gc})}{C_{gw}} = \frac{(U - C_{gc})}{\sqrt{g\Delta\theta h_o/\theta_{vw}}}$$

- U = mean wind speed of ambient air below density current height
- C_{gc} = adjusted speed of gravity current (Liu & Moncrieff 1996)
  - I also estimated C_{gc} using a cold pool tracking method
- C_{th} = theoretical (densimetric) speed of gravity current
  - ρ_w = density of ambient air
  - ρ_c = density of cold pool (GC)
  - $\mu = 0.75$
  - $U_o = U$
- d_o = depth of gravity current (Used 5 methods)
  - θ_{vw} = virtual potential temperature of ambient air
  - θ_{vc} = virtual potential temperature of cold pool (GC)
  - $\Delta p = p_c - p_w$
- C_{gw} = speed of gravity wave
  - $\Delta\theta = \theta_{invtop} - \theta_{invbottom}$
  - θ_v = mean virtual potential temperature of ambient air below the inversion
  - h_o = inversion height – level at which $d\theta/dz < 0.005$ K/m

$$C_{gc} = C_{th} + \mu U_o$$

$$C_{th} = \sqrt{g d_o \frac{\rho_c - \rho_w}{\rho_w}}$$

$$d_o = \frac{\Theta_{vc}\Delta p}{\rho_w g[(p_c/p_w)\Theta_{vw} - \Theta_{vc}]}$$

$$C_{\mathrm{gw}} = \left[g\left(\frac{\Delta\theta_v}{\theta_v}\right)h_0\right]^{1/2}$$

Scorer Parameter

Taylor-Goldstein Equation

$$m^2 = \underbrace{\frac{N_m^2}{(U - C_{bore})^2} - \frac{\partial^2 U/\partial z^2}{(U - C_{bore})}}_{l^2} - k^2$$

m = vertical wavenumber
k = horizontal wavenumber

- A sufficient wave duct is needed to trap wave energy and prevent the vertical propagation of energy out of the stable layer (Lindzen & Tung 1976)
  - Upper level winds oppose the wave motion
  - LLJ at low levels opposes the wave motion
  - Inversion above the lower stable layer – energy can be reflected off the inversion for certain inversion heights
- Scorer parameter (l^2) used to diagnose the probability of a wave duct (Scorer 1949; Crook 1988)
- If l^2 decreases with height, reflection will occur and some of the wave energy will be trapped
- If $l^2 < 0$ at some height, all vertically propagating waves below that level will be trapped

Methods

- In order to generate bores, we need:
  - Partially or completely blocked flow regime
  - Presence of μ layer: where μ > 0.7
  - Presence of a wave duct: layer of negative Scorer above positive Scorer
- Obtained two soundings:
  - ambient air ahead of gravity current (≥ 10 km ahead of leading edge)
  - gravity current (≥ 10 km behind the leading edge)
- Calculated F, l^2, etc. using 5 d_o methods for 6 propagation angles (21°, 0°, 344°, 330°, 315°, 293°) at 5 different times (0930, 0945, 10, 1015, 1030 UTC)

$$F = \frac{(U - C_{gc})}{C_{gw}} = \frac{(U - C_{gc})}{\sqrt{g\Delta\theta h_o/\theta_{vw}}}$$

$$C_{gc} = C_{th} + \mu U_o$$

$$C_{th} = \sqrt{g d_o \frac{\rho_c - \rho_w}{\rho_w}}$$

$$d_o = \frac{\Theta_{vc}\Delta p}{\rho_w g[(p_c/p_w)\Theta_{vw} - \Theta_{vc}]}$$

$$C_{\mathrm{gw}} = \left[g\left(\frac{\Delta\theta_v}{\theta_v}\right)h_0\right]^{1/2}$$

$$\mu = \frac{C_0}{C_{gc}} = \frac{2Nh_0/\pi}{C_{gc}}$$

$$m^2 = \underbrace{\frac{N_m^2}{(U - C_{bore})^2} - \frac{\partial^2 U/\partial z^2}{(U - C_{bore})}}_{l^2} - k^2$$

0^{o} Region 1015 UTC

Method	Avg d_o depth (m)
TH	833.95
INV	1218.95
WS	1332.3
HYD	1255.64
HYB	1274.76
EST	**1000**

Method	Avg C_{gc} Speed ($m\ s^{-1}$)
TH	3.78
INV	6.29
WS	6.72
HYD	6.24
HYB	6.39
EST	**13.33**

- d_o depths in agreement and reasonable
- Partially blocked flow regime
- GC speeds consistent but underpredicted (used EST for all points on diagram)
- Sufficient wave ducts

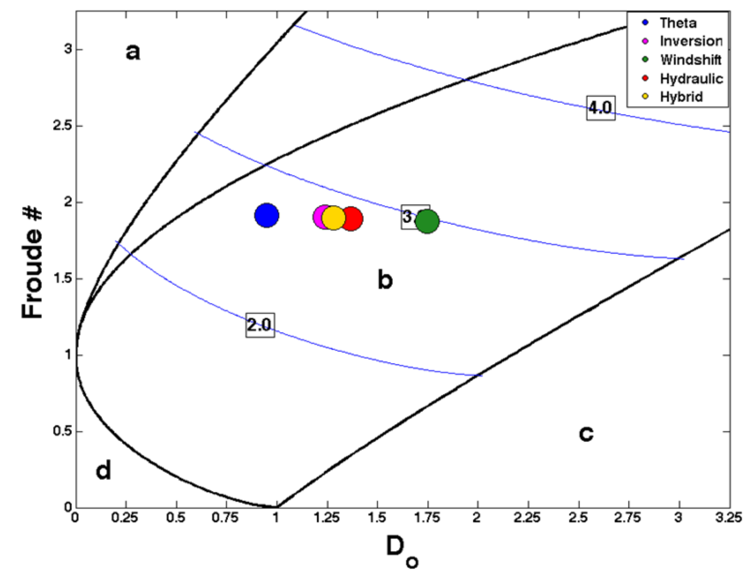

Figure courtesy of Kevin Haghi

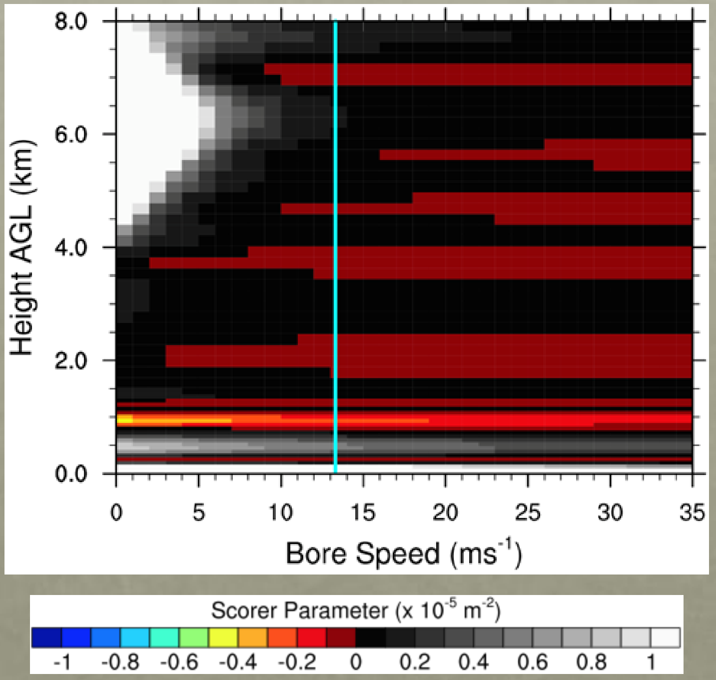

315° Region 1015 UTC

Method	Avg d_o depth (m)
TH	438.6
INV	1343.7
WS	3324.97
HYD	4056.09
HYB	2588.19
EST	1300

Method	Avg C_{gc} Speed (m s^{-1})
TH	-1.8
INV	3.18
WS	11.81
HYD	14.62
HYB	8.97
EST	15.71

- d_o depths diverge and are unrealistic
- Partially or completely blocked flow regime
- GC speeds inconsistent (used EST for all)
- Wave ducts present at low levels but not aloft

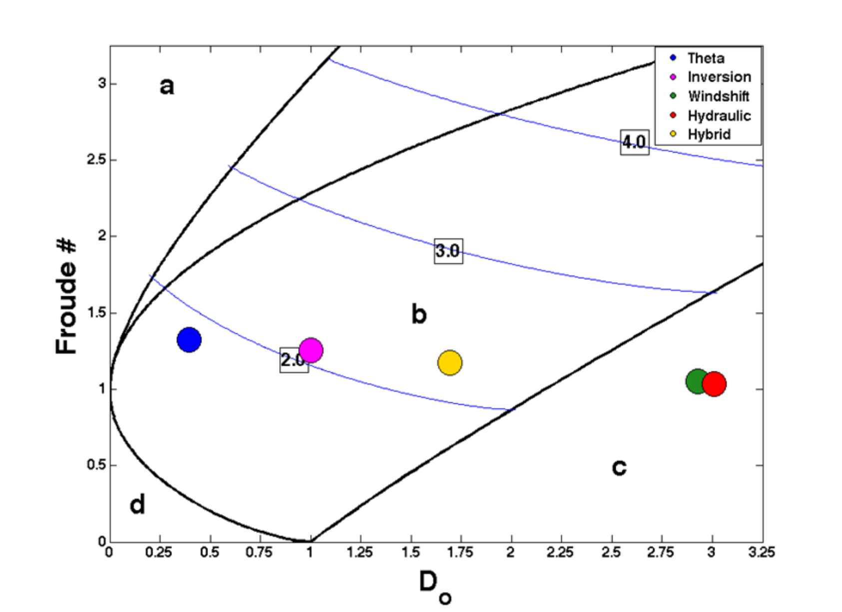

Figure courtesy of Kevin Haghi

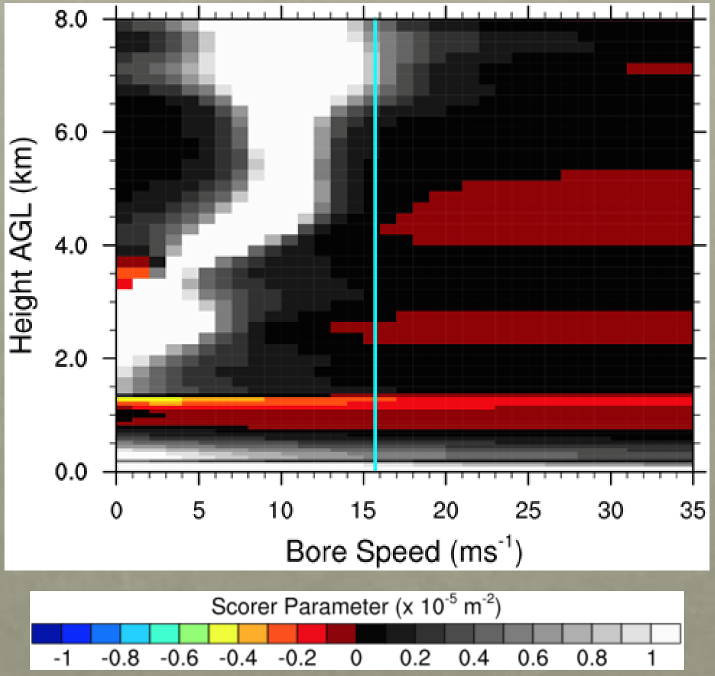

Scorer Parameter 13Z

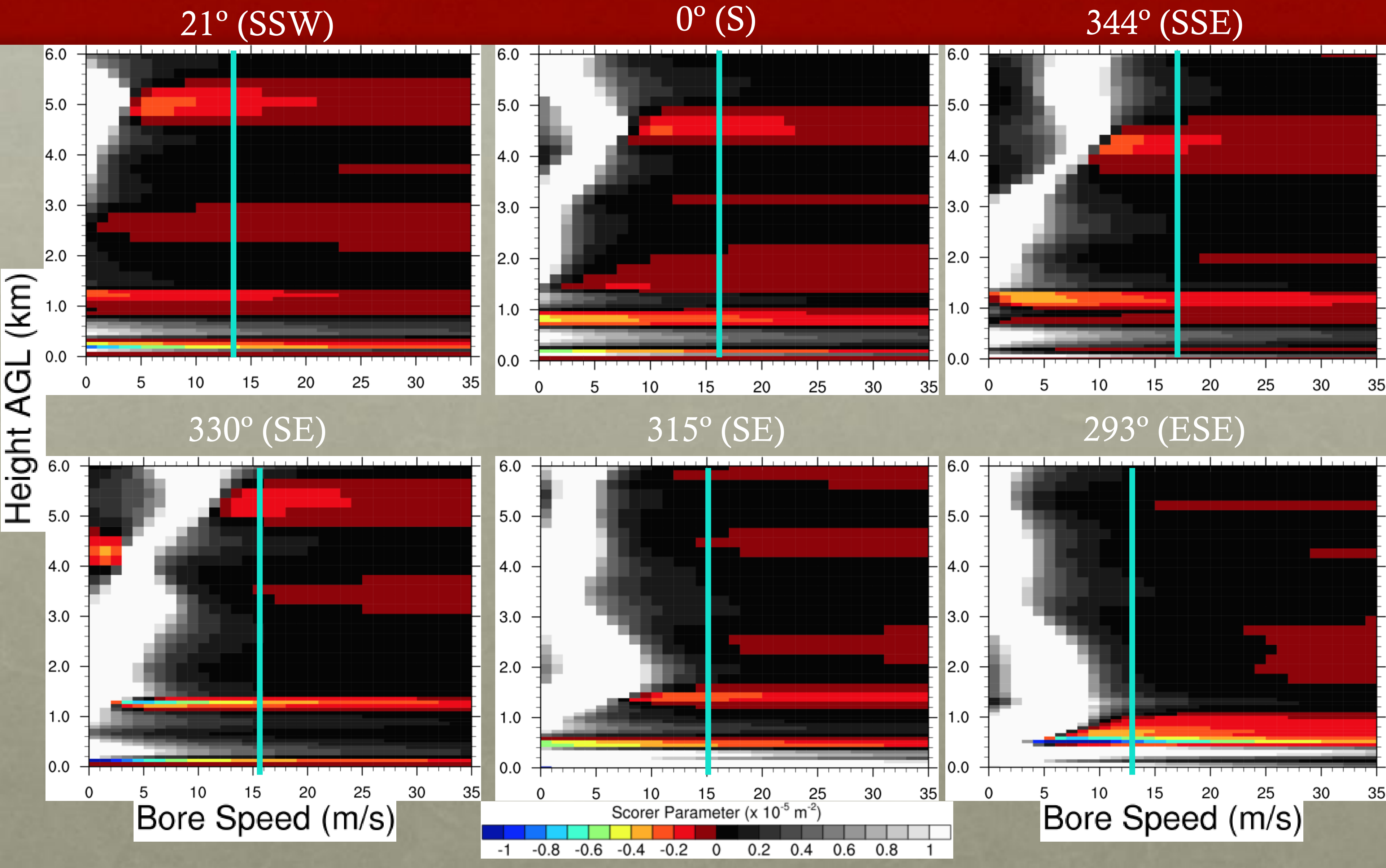

Summary
Wave Theory Framework

- Vertical profile of wave trapping is complicated with multiple ducting layers and significant variations around the cold pool
- Predictions of GC depths in agreement on southern end but not on eastern end
  - Deep ascent of stable air occurring on the eastern side – wave extends back into cold pool, causes d_o methods to diverge
- C_{gc} often unrealistic – speed should be estimated using cold pool tracking method (observed C_{gc})
- Froude # indicates partially blocked flow occurring in all 6 regions
  - Not surprising, as gravity currents tend to produce blocked flow in the nocturnal environment (Haghi and Parsons 2016)
- Convection continues on southeast end
  - Deep ascent is what's more important in maintaining convection at night – can be initiated by a bore but don't want a long-lived undular bore trapped at low levels – bore remains close to cold pool with deeper ascent at the leading edge

Conclusions

- WRF does an adequate job at recreating the storm and its environment
- Convective feedbacks associated with bores/waves with leaky ducts, weak surface cold pools, and advection by the LLJ are likely responsible for nocturnal convection (south of the front)
- Nighttime convection with a SBL is quite different; deep lifting of stable air needs to occur
- Lifting creates additional buoyancy gradients responsible for the surging forward of systems
- Lifting varies along the highly 3D outflow
- Local measurements limit one's ability to understand these systems

- Field campaign involving several agencies (NSF, NOAA, NASA, DOE) designed to further the understanding of continental nocturnal warm-season precipitation

- Field Phase: June 1 – July 15 2015

- Main objective was to gather observational evidence to support theories for initiation, maintenance, and prediction of nocturnal convection

Future Work (time-permitting)

- Microphysics parameterization schemes
- Consider resonance of bores and waves
  - If a critical layer exists above the wave duct and possesses a $Ri \leq 0.25$, wave reflection can occur
- Initialize case with NAM data
- Re-run case with the NMMB model
- Apply theory developed herein to more cases

Acknowledgements

Dr. David Parsons
Advisor

Dr. Alan Shapiro
Committee
Member

Dr. Xuguang Wang
Committee
Member

Kevin Haghi
PhD Candidate

- Also special thanks to Larissa Reames, Manda Chasteen, Kelton Halbert, Dylan Reif, Chris Riedel, and Dr. Steven Cavallo for all of their suggestions and input to this work!

Terra Incognita

- Grid spacing of 1-km chosen for inner domain in order to more accurately represent turbulent, microphysical, and convective processes at night

- 1-km grid spacing lies in the numerical gray zone for boundary layer processes, or terra incognita (Wyngaard 2004)
  - Where the grid spacing of a NWP model is comparable to the dominant length scale of the flow

- During the day, turbulence in the PBL can span its entire depth (~1-2 km)
  - Unclear whether PBL parameterization schemes should be employed

- During stable conditions at night, dominant length scale of PBL flow changes to around 100 m or less (Stull 1988)

- **While 1-km grid spacing lies in the gray zone during the day, it does not at night** (Zhou et al. 2014)

2200 UTC

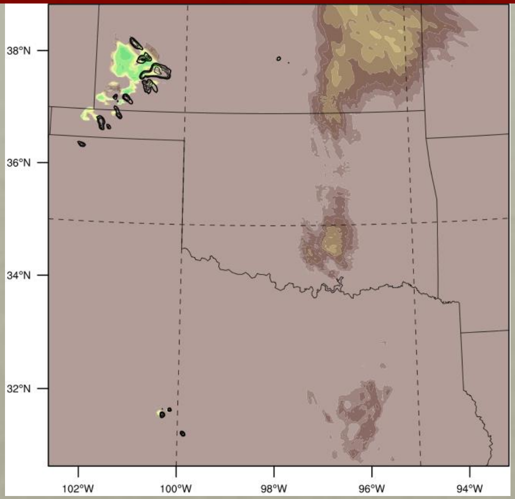

0900 UTC

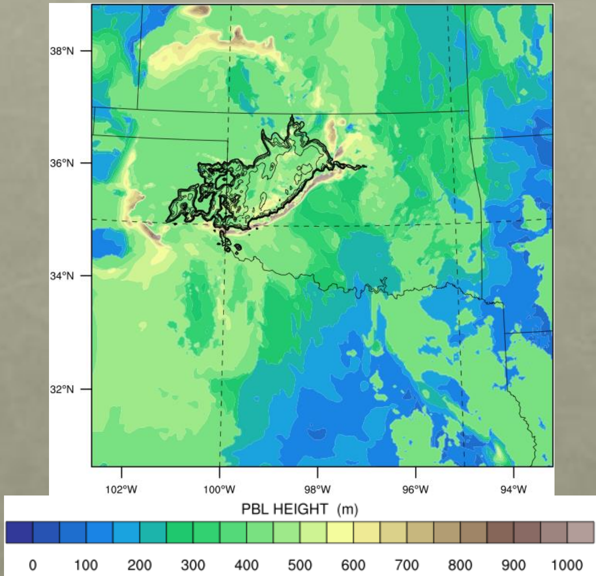

Sensitivity Tests
Microphysics schemes

1300 UTC

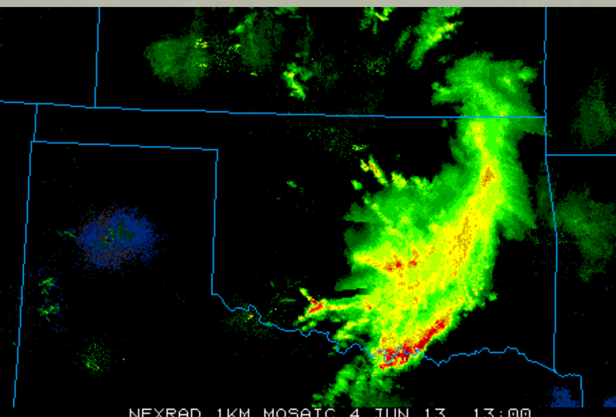

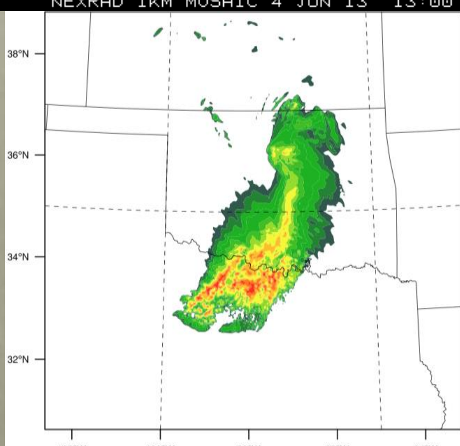

WSM6 Scheme

0400 UTC

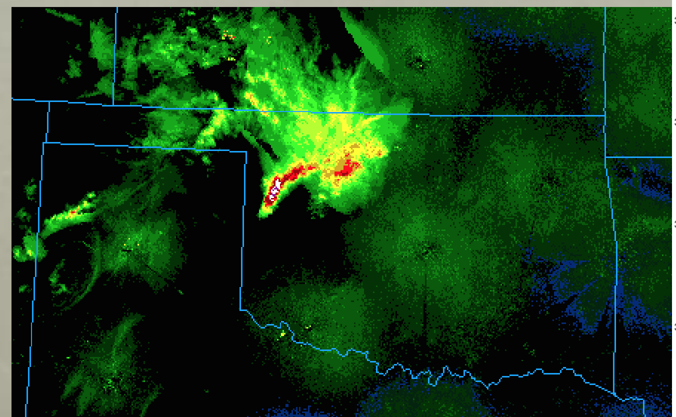

NSSL Scheme

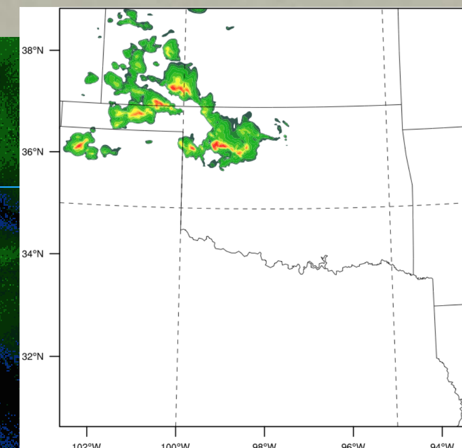

0730 UTC

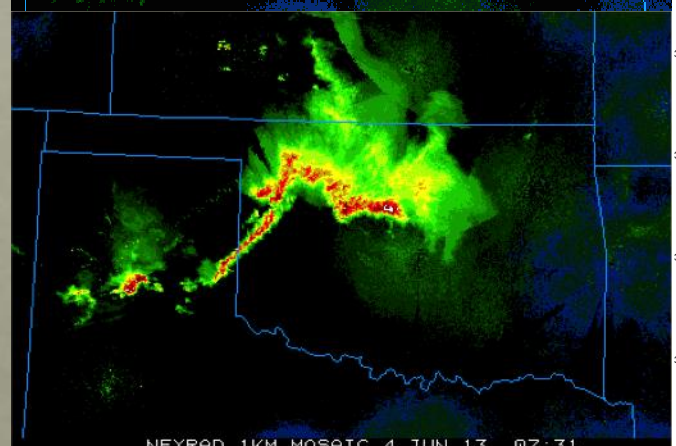

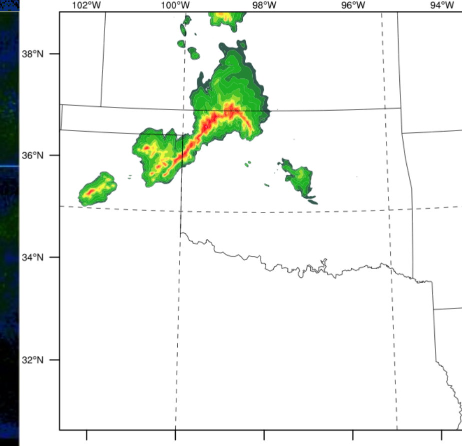

Sensitivity Tests
PBL schemes

- MYJ – produced nonexistent convection, did not capture transition well

Observed Reflectivity (dBZ)

MYJ Reflectivity (dBZ)

2300 UTC

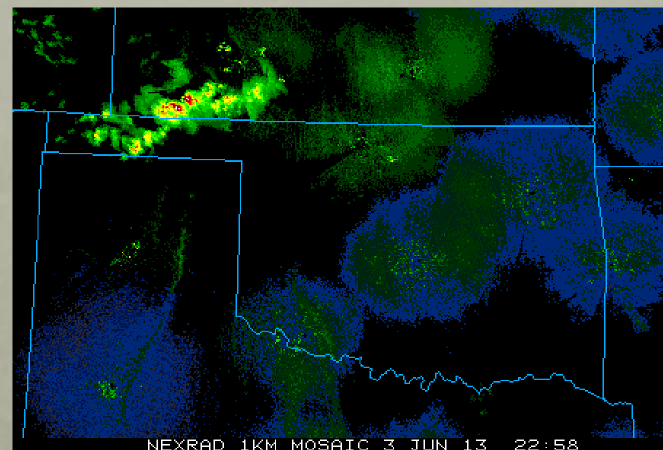

0730 UTC

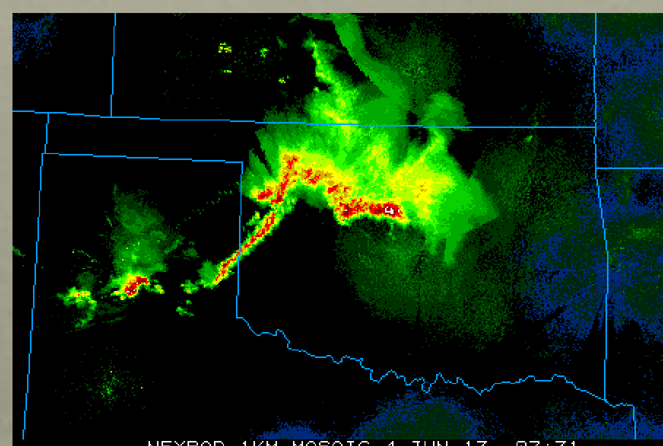

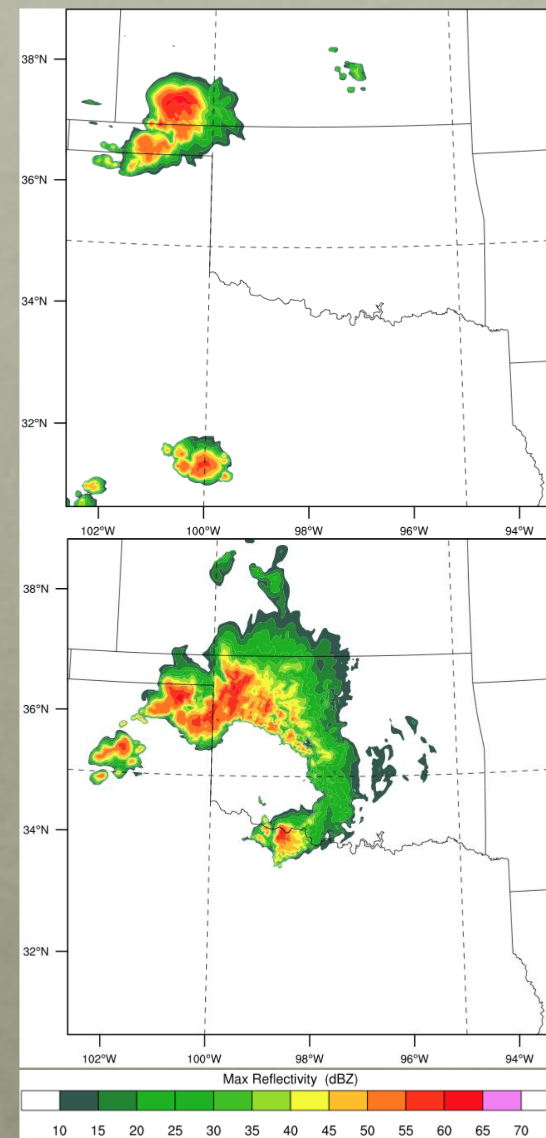

Sensitivity Tests PBL schemes

- YSU – produced a warm surface temperature bias

YSU

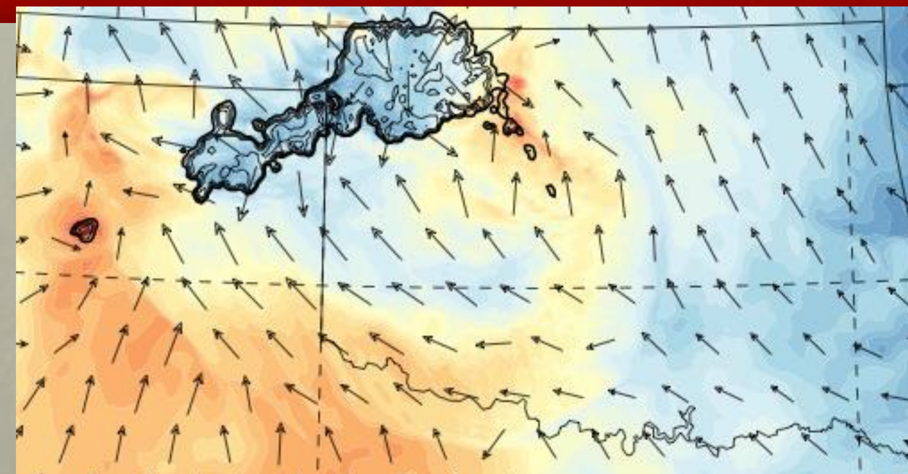

Mesonet

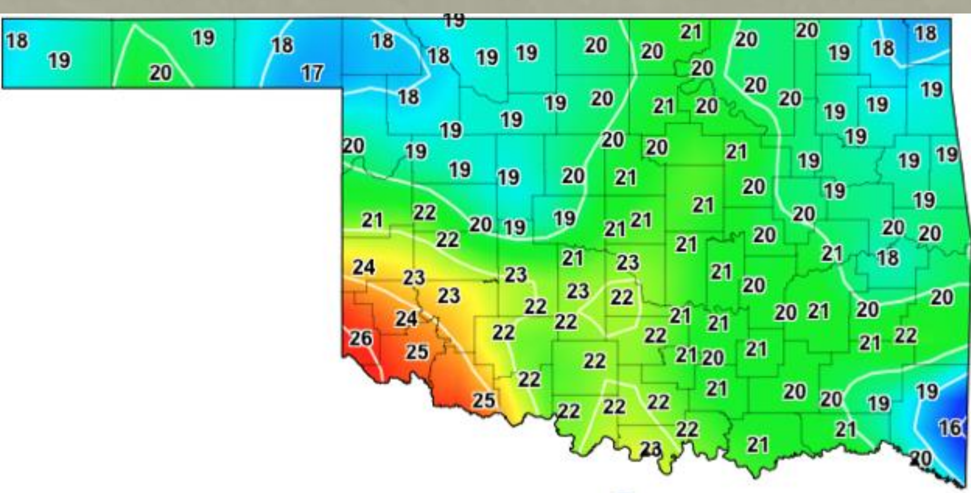

MYNN

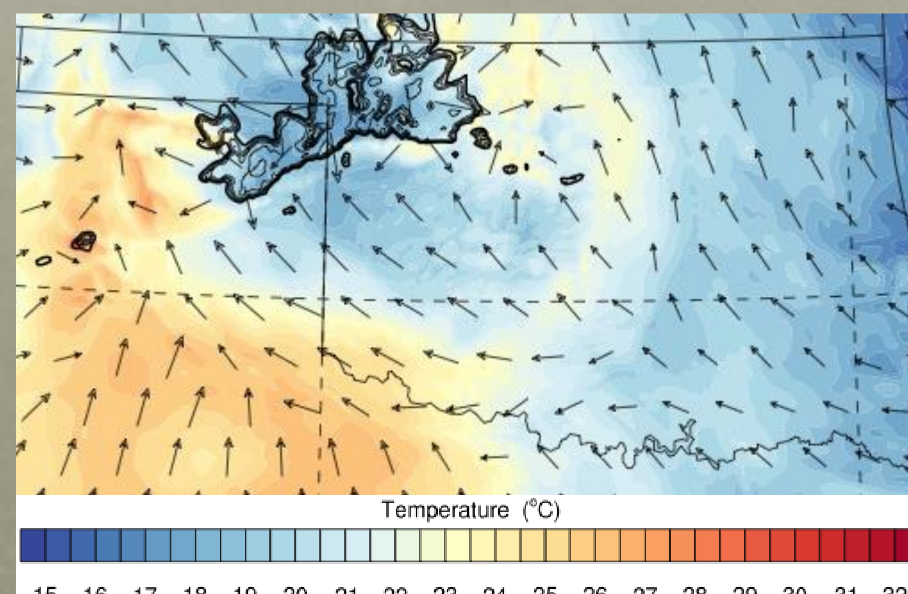

Sensitivity Tests
GFS Model Run

Observed Reflectivity (dBZ) | RAP Reflectivity (dBZ) | GFS Reflectivity (dBZ)

0730 UTC

1500 UTC

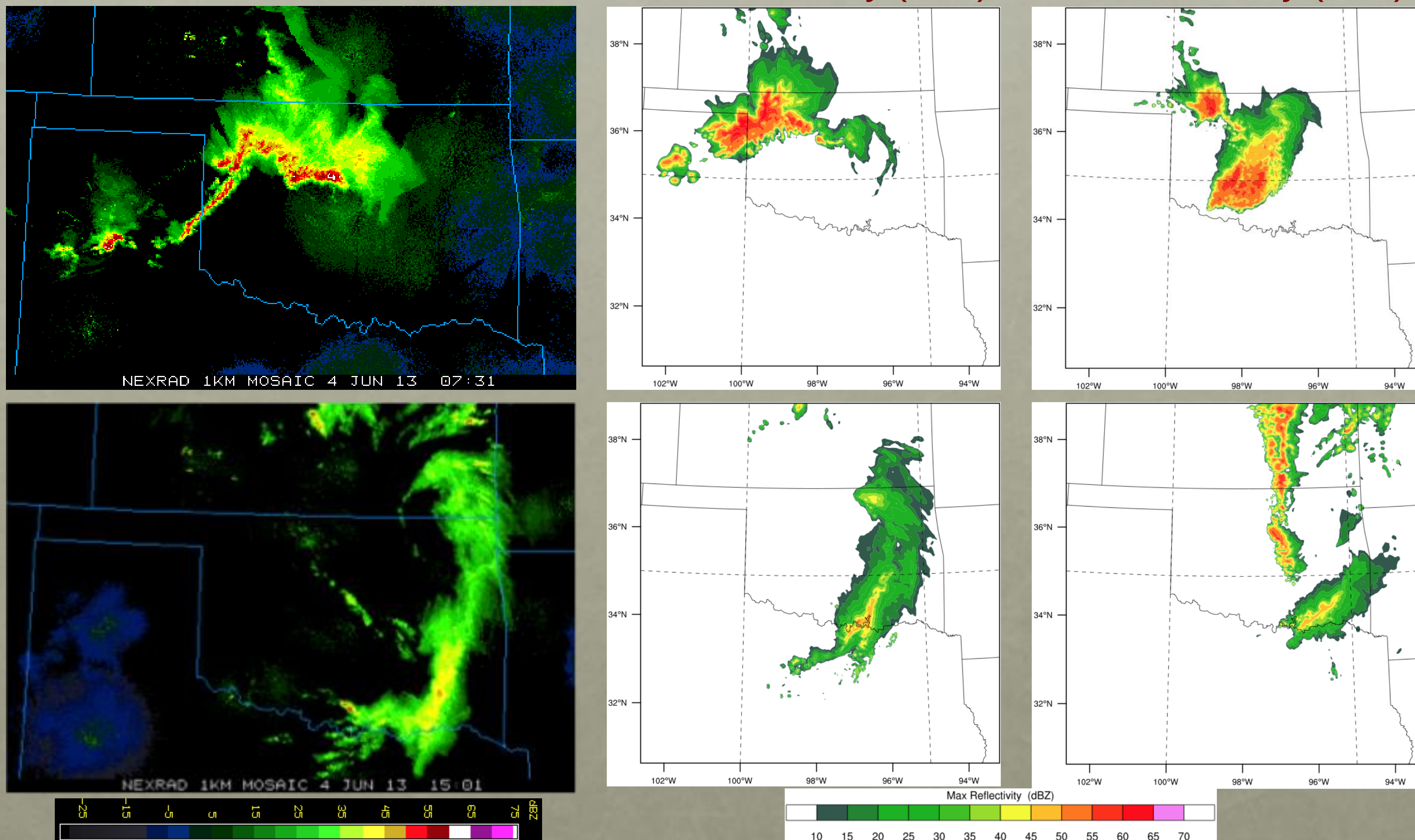

Buoyancy Gradients Generate Internal Circulations

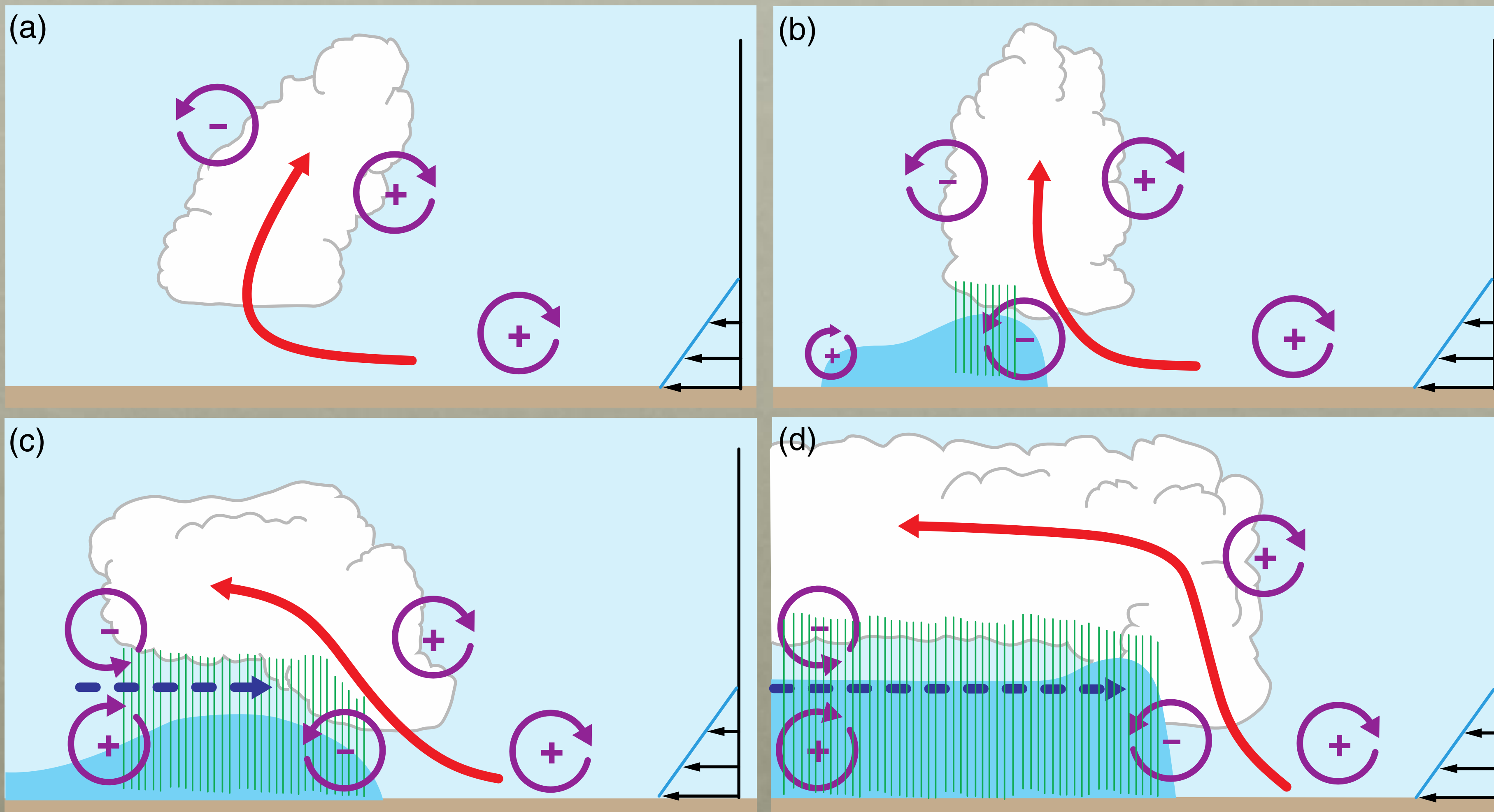

Figure courtesy of SUNY Albany

Uncertainty in Gravity Current Depth

- Hydraulic Method
  - Use surface θ for ambient air and gravity current air
- Theta Method
  - Model level above gravity current air where θ becomes greater than surface θ for ambient air
- Hybrid Method
  - Use mean θ up to gravity current top predicted by the theta method for both θ's
- Inversion Method
  - Inversion height of gravity current air –level at which dθ/dz < 0.005 K/m – layer must be at least 200 m thick
- Windshift Method
  - Level at which ground relative wind in cross section changes direction

$$d_o = \frac{\Theta_{vc}\Delta p}{\rho_w g[(p_c/p_w)\Theta_{vw} - \Theta_{vc}]}$$

Methods used by Kevin Haghi in real-time to predict bores for PECAN

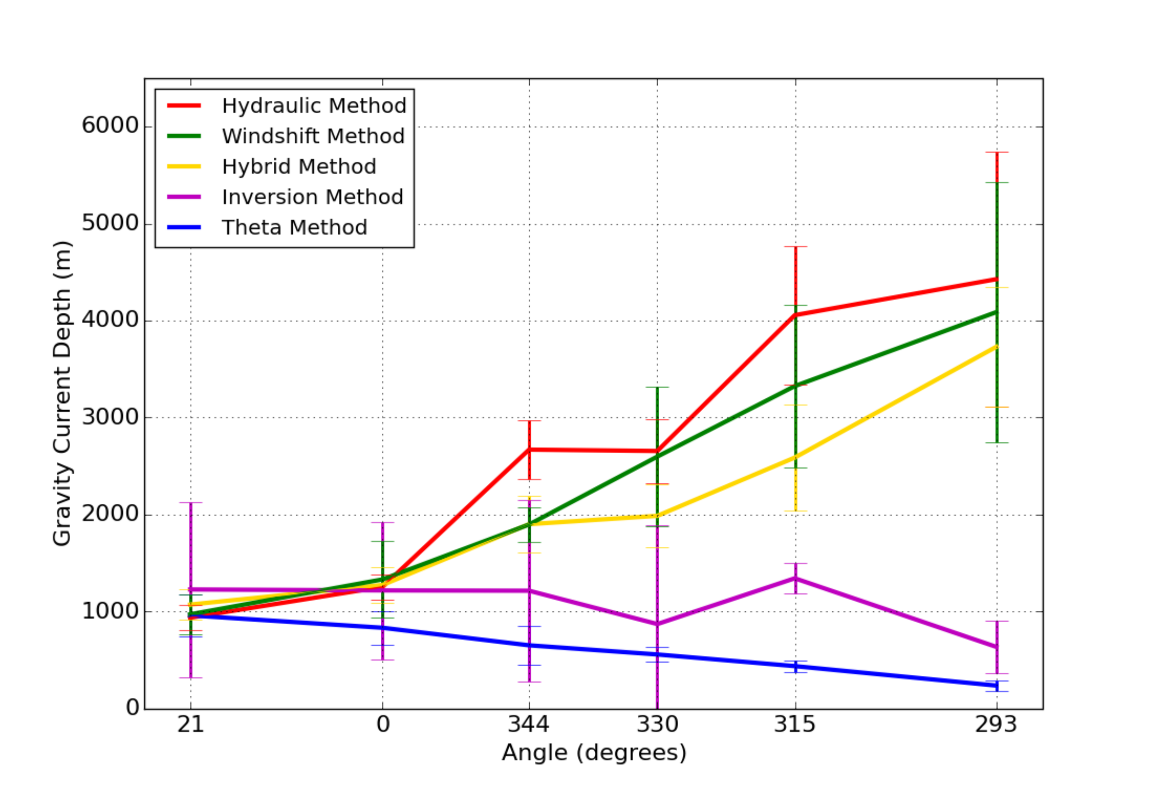

Note: Angle corresponds to the direction which the feature is coming from

Bore Strength, Bore Depth, Bore Speed

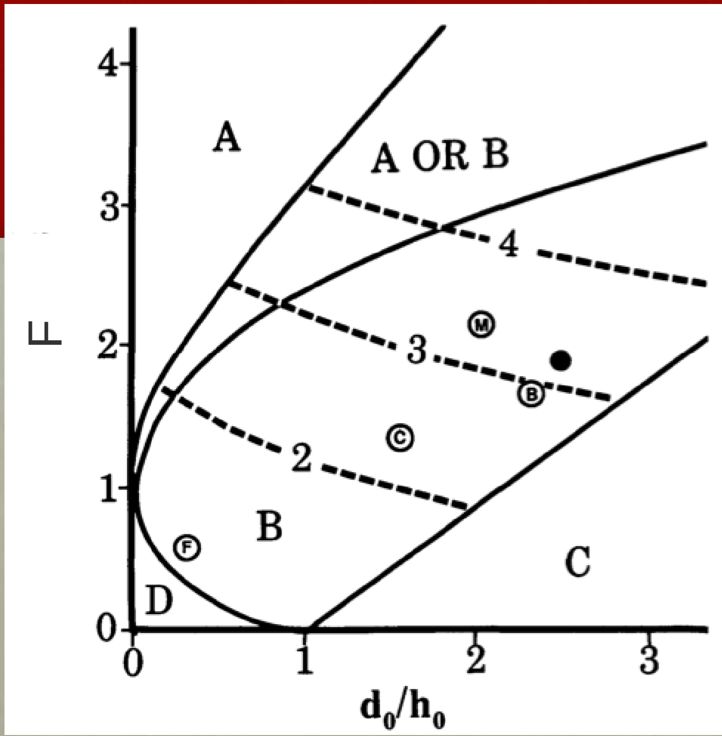

- Bore Strength: the ratio of the bore depth (h_1) to the inversion height (h_o)
  - Indicated by dashed lines on figure (from Koch et al. 1991)

$$bstr = \frac{h_1}{h_0}$$

- Bstr determined by solving the system of 3 equations
- Predicted Bore Speed (C_{bore})
  - If bstr > 2, use
  - If bstr ≤ 2, use

$$C_{bore} = C_{gw} * 1.19 * bstr^{0.5}$$

$$\frac{C_{bore}}{C_{gw}} = (0.5 * bstr * (1 + bstr))^{0.5}$$

$$\frac{u_1}{C_{gw}} = F - ((1 - bstr^{-1}) * \frac{C_{bore}}{C_{gw}})$$

$$bstr = D_o - (0.5 * (\frac{u_1}{C_{gw}})^2) + 1.5(bstr * \frac{u_1}{C_{gw}})^{\frac{3}{2}}$$

- C_{bore} defined as bore speed in a reference frame in which the upstream fluid is at rest (Rottman and Simpson 1989)
- Mean wind speed of ambient air beneath predicted bore height (h_1) was subtracted from C_{bore}